A novel 16-Hydroxy-Palmitic Acid tethered D-configured Homo-chiral Triphenylalanine based Nanofibrillar Scaffold with innate anticancer potential

Vaibhav Shivhare,[a] Arindam Gupta,[b] Rishabh Ahuja,[a] Dipesh Barde,[a] Surendra Kumar Ahirwar,[a] Anindya Basu [c,d] and Anita Dutt Konar *[a,c,d]

Synthesis of Compounds

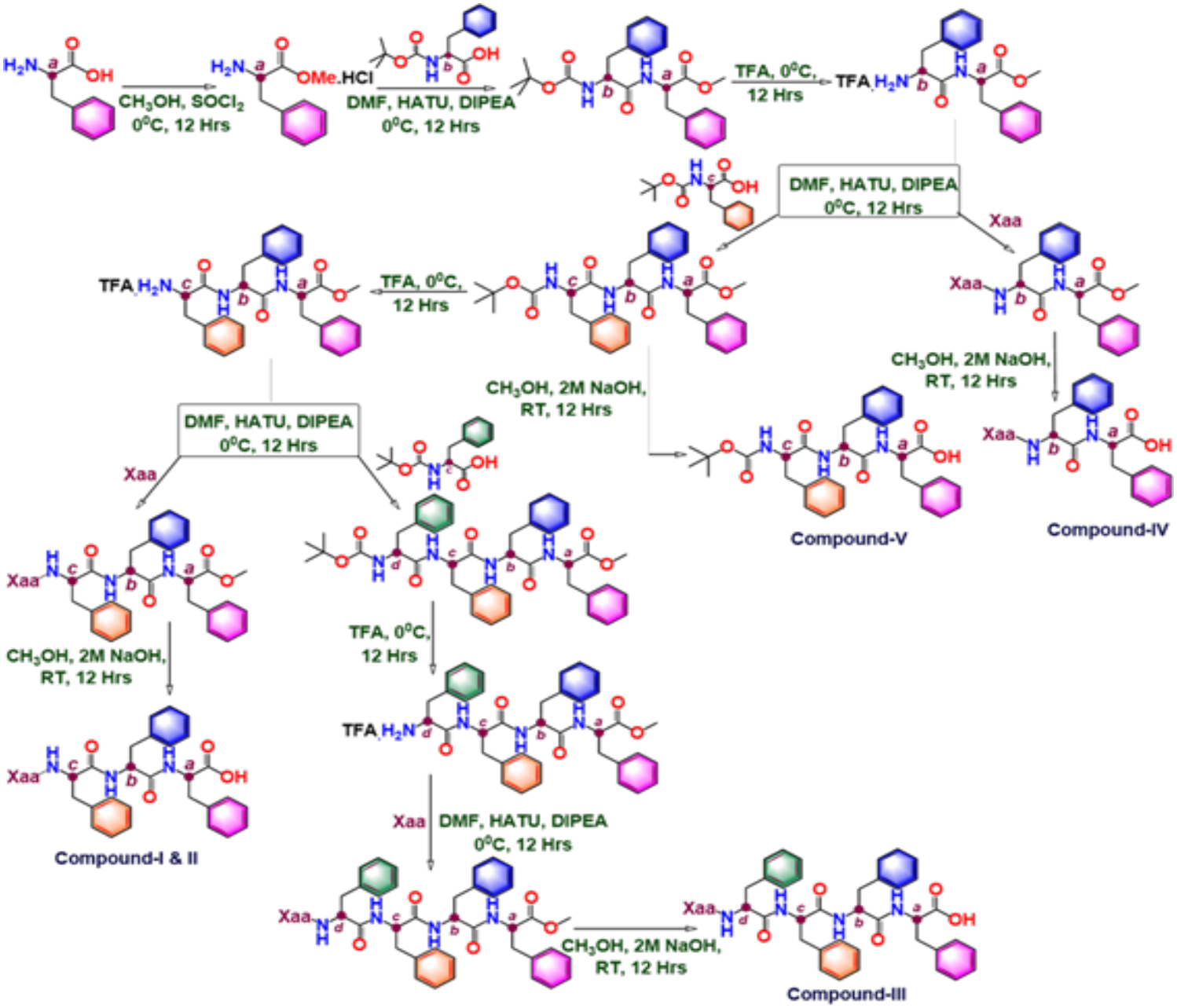

Scheme of Compounds (I-V)		a)	b)	c)	d)
Xaa = 12-Hydroxy palmitic acid	Compound I	D	D	D	-
	Compound II	L	L	L	-
	Compound III	D	D	D	D
	Compound IV	D	D	-	-
Boc-D(Phe)-D(Phe)-OH	Compound V	D	D	D	-

Scheme S1: - Synthesis Scheme for Compounds **I-V**

S. No.	Compounds	Structure
01.	Compound-I	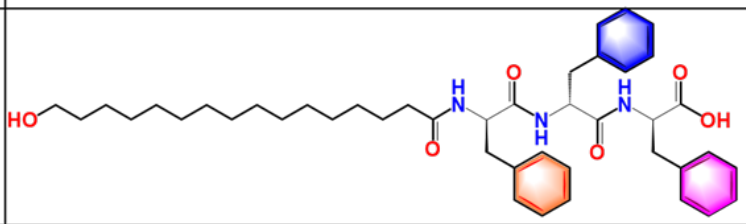
02.	Compound-II	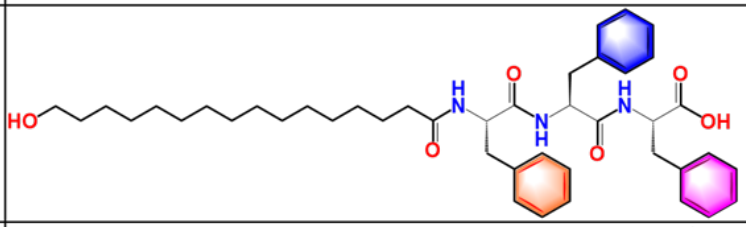
03.	Compound-III	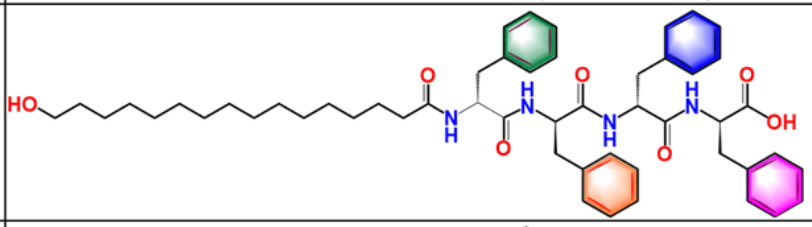
04.	Compound-IV	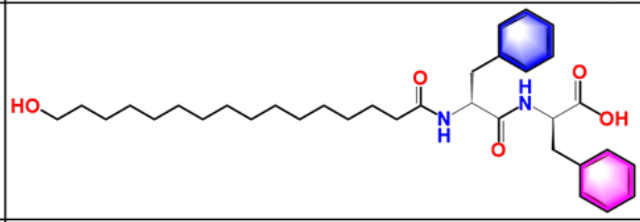
05.	Compound-V	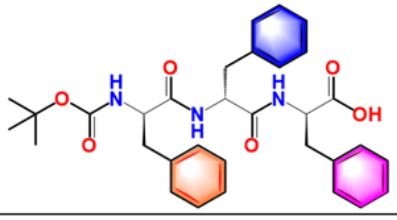

Figure S1: Detailed Structures of Compounds **I-V**

Experimental Techniques Adopted

Synthesis of the Compounds: Conventional solution phase methodology was employed in order to synthesize the compounds with racemization free techniques as described in the Scheme as follow. Thin Layer Chromatography (TLC) on silica gel was used to check the purity of the obtained intermediates. The final products were purified through column chromatography by silica gel (100-200 mesh) as the stationary phase and the mixture of ethyl acetate and petroleum ether as the eluent.

Synthesis of the dipeptides: Boc-(Y)-Phe-(Z)-Phe-OMe: The **Z**-Phe-OMe obtained from its hydrochloride (Z=D; 12.16 gm, 56.60 mmol) or (Z=L; 3 gm, 11.32 mmol) was added to an ice cold solution of Boc-**Y**-Phe-OH (Y=D; 15 gm, 56.60 mmol) or (Y=L; 2.43 gm, 11.320 mmol) in 25 ml of DMF. Then HATU (D-Phe; 21.50 gm, 56.60 mmol) or (L-Phe; 4.3 gm, 11.32 mmol): Hexafluorophosphate Azabenzotriazole Tetramethyl Uronium) was added to the cooled mixture, which was stirred for 18 hours in ice cold condition. The progress of the reaction was monitored by TLC. The

residue was taken into ethyl acetate. The organic layer was washed with 2 M HCl (3 × 100), 1 M Sodium carbonate (3 × 100 ml) and brine (2 × 100 ml), dried over anhydrous sodium sulphate and evaporated in *vacuum* to obtain a white solid material. The crude peptide was used without further purification.

Yield:

a. Y=D; Z=D: 20.51 g (48.08 mmol, 85 %) **(Molecule-I)**

b. Y=L; Z=L: 4.32 g (10.12 mmol, 90 %) **(Molecule-II)**

Synthesis of Boc-(X)-Phe-(Y)-Phe-(Z)-Phe-OMe: The crude peptide **Molecule-(I)** (12 gm, 28.13 mmol) or **Molecule-(II)** (4.32 gm, 10.12 mmol) was treated with TFA at 0^{o}C and allow to stirred for overnight. without further purification. The progress of the reaction was monitored by TLC. The Reaction mixture was diluted with Water and allow to cool at room temperature then Organic solvent was added. Anhydrous Sodium bicarbonate powder was added to neutralize the reaction. Organic layer was separated using separating funnel and dried over using anhydrous Sodium sulphate. The organic layer was used directly to the further reaction. +**Y**-Phe-**Z**-Phe-OMe obtained was added to an ice cold solution of Boc-**X**-Phe-OH (X=D; 7.45 gm, 28.13 mmol) or (X=L; 2.68 gm, 10.12 mmol) in 15 ml of DMF. Then HATU (D-Phe; 10.68 gm, 28.13 mmol) or (L-Phe; 3.84 gm, 10.12 mmol): Hexafluorophosphate Azabenzotriazole Tetramethyl Uronium) was added to the cooled mixture, which was stirred for 18 hours in ice cold condition. The progress of the reaction was monitored by TLC. The organic layer was washed with 2 M HCl (3 × 100), 1 M Sodium carbonate (3 × 100 ml) and brine (2 × 100 ml), dried over anhydrous sodium sulphate and evaporated in *vacuum* to obtain a white solid material. (Boc-**X**-Phe-**Y**-Phe-**Z**-Phe-OMe was obtained)

c. X=D; Y=D; Z=D: 14.52 g (25.30 mmol, 90 %) **(Molecule-III)**

d. X=L; Y=L; Z=L: 4.64 g (8.08 mmol, 80 %) **(Molecule-IV)**

Synthesis of Boc-(W)-Phe-(X)-Phe-(Y)-Phe-(Z)-Phe-OMe: The crude peptide **[Molecule-III]** (3 gm, 5.22 mmol) was treated with TFA at 0^{o}C and allow to stirred for overnight. without further purification. The progress of the reaction was monitored by TLC. The Reaction mixture was diluted with Water and allow to cool at room temperature then Organic solvent was added. Anhydrous Sodium bicarbonate powder was added to neutralize the reaction. Organic layer was separated using separating funnel and dried over using anhydrous Sodium sulphate. The organic layer was used directly to the further reaction. +**X**-Phe-**Y**-Phe-**Z**-Phe-OMe obtained was added to an ice cold solution of Boc-**W**-Phe-OH (1.38 gm, 5.22 mmol) in 15 ml of DMF. Then HATU (1.98 gm, 5.22 mmol: Hexafluorophosphate Azabenzotriazole Tetramethyl Uronium) was added to the cooled mixture, which was stirred for 18 hours in ice cold condition. The progress of the reaction was monitored by TLC. The organic layer was washed with 2 M HCl (3 × 100), 1 M Sodium carbonate (3 × 100 ml) and brine (2 × 100 ml), dried over anhydrous sodium sulphate and evaporated in *vacuum* to obtain a white solid material. (Boc-**W**-Phe-**X**-Phe-**Y**-Phe-**Z**-Phe-OMe was obtained)

e. W=D; X=D; Y=D; Z=D: 3.38 g (4.68 mmol, 90 %) **(Molecule-IX)**

Synthesis of 16-Hydroxypalmitic acid-(Y)-Phe-(Z)-Phe-OMe: To Boc-(Y)-Phe-(Z)-Phe-OMe [Molecule I] (3 gm, 7.03 mmol) (the exact amount obtained from the above step) trifluoroacetic acid (12 ml, minimum amount) was added at 0^0C and the mixture was stirred at room temperature. The removal of the Boc group was monitored by TLC. After 12 h the trifluoroacetic acid was removed under reduced pressure to afford the crude trifluoroacetate salt. This dipeptide salt was treated with $NaHCO_3$ and extracted by ethyl acetate, and added to an ice-cold solution of **16-Hydroxypalmitic acid** (1.91 gm, 7.03 mmol) in 10 ml of DMF. Then HATU (2.67 gm, 7.03 mmol: Hexafluorophosphate Azabenzotriazole Tetramethyl Uronium) added to the cooled mixture, which was stirred for 18 hours in ice cold condition. The progress of the reaction was monitored by TLC. The residue was taken into ethyl acetate. The organic layer was washed with 2 M HCl (3 × 100), 1 M Sodium carbonate (3 × 100 ml) and brine (2 × 100 ml), dried over anhydrous sodium sulphate and evaporated in *vacuum* to obtain a white solid material. The crude peptide was used without further purification.

Yield: **16-Hydroxypalmitic acid**-(Y)-Phe-(Z)-Phe-OMe

a. Y=D; Z=D: 3.26 g (5.61 mmol, 80 %) **(Molecule-V)**

Synthesis of 16-Hydroxypalmitic acid-(X)-Phe-(Y)-Phe-(Z)-Phe-OMe: To **[Molecule III]** (3 gm, 5.22 mmol) or **[Molecule IV]** (4.64 gm, 8.08 mmol) (the exact amount obtained from the above step) trifluoroacetic acid (12 ml, minimum amount) was added at 0^0C and the mixture was stirred at room temperature. The removal of the Boc group was monitored by TLC. After 12 h the trifluoroacetic acid was removed under reduced pressure to afford the crude trifluoroacetate salt. This dipeptide salt was treated with $NaHCO_3$ and extracted by ethyl acetate, and added to an ice-cold solution of **16-Hydroxypalmitic acid** (D-Phe; 1.42 gm, 5.22 mmol) or (L-Phe; 2.2 gm, 8.08 mmol) in 25 ml of DMF. Then HATU (D-Phe; 1.98 gm, 5.22 mmol) or (L-Phe; 3.07 gm, 8.08 mmol): Hexafluorophosphate Azabenzotriazole Tetramethyl Uronium) added to the cooled mixture, which was stirred for 18 hours in ice cold condition. The progress of the reaction was monitored by TLC. The residue was taken into ethyl acetate. The organic layer was washed with 2 M HCl (3 × 100), 1 M Sodium carbonate (3 × 100 ml) and brine (2 × 100 ml), dried over anhydrous sodium sulphate and evaporated in *vacuum* to obtain a white solid material. The crude peptide was used without further purification.

Yield: **16-Hydroxypalmitic acid**-(X)-Phe-(Y)-Phe-(Z)-Phe-OMe

b. X=D; Y=D; Z=D: 2.85 g (3.91 mmol, 75 %) **(Molecule-VI)**

c. X=L; Y=L; Z=L: 6.009 g (6.86 mmol, 85 %) **(Molecule-VII)**

Synthesis of 16-Hydroxypalmitic acid-(W)-Phe-(X)-Phe-(Y)-Phe-(Z)-Phe-OMe: To [Molecule IX] (3.38 gm, 4.68 mmol) (the exact amount obtained from the above step) trifluoroacetic acid (12 ml, minimum amount) was added at 0^0C and the mixture was stirred at room temperature. The removal of the Boc group was monitored by TLC. After 12 h the trifluoroacetic acid was removed under reduced pressure to afford the crude trifluoroacetate salt. This dipeptide salt was treated with $NaHCO_3$ and extracted by ethyl acetate, and added to an ice-cold solution of **16-Hydroxypalmitic acid** (1.27 gm,

4.68 mmol) in 20 ml of DMF. Then HATU (1.77 gm, 4.68 mmol: Hexafluorophosphate Azabenzotriazole Tetramethyl Uronium) added to the cooled mixture, which was stirred for 18 hours in ice cold condition. The progress of the reaction was monitored by TLC. The residue was taken into ethyl acetate. The organic layer was washed with 2 M HCl (3 × 100), 1 M Sodium carbonate (3 × 100 ml) and brine (2 × 100 ml), dried over anhydrous sodium sulphate and evaporated in *vacuum* to obtain a white solid material. The crude peptide was used without further purification.

Yield: **16-Hydroxypalmitic acid**-(X)-Phe-(Y)-Phe-(Z)-Phe-OMe

- **a.** X=D; Y=D; Z=D: 3.27 g (3.73 mmol, 80 %) **(Molecule-X)**

Synthesis of 16-Hydroxypalmitic acid-(X)-Phe-(Y)-Phe-(Z)-Phe-OH: [Molecule-VI] (2.85 gm, 3.91 mmol) or **[Molecule-VII]** (6.009 gm, 8.25 mmol) was dissolved in calculated amount of methanol ***(***20 ml***)*** and NaOH ***(***2M NaOH***:*** 14 ml***)*** was added dropwise to the solution**.** The progress of the reaction was monitored by TLC**.** After completion of the reaction, as determined by TLC, the methanol was evaporated**.** The residue containing the sodium salt was dissolved in water and extracted with diethyl ether to remove the unreacted stuff**.** The aqueous layer obtained was cooled, acidified with 2N HCl and extracted with ethyl acetate**.** The solvent was evaporated *in vacuo* to obtain a white solid**.**

Yield: 16-Hydroxypalmitic acid-**(**X**)**-Phe-**(**Y**)**-Phe-**(**Z**)**-Phe-OH

- **a.** X=D; Y=D; Z=D: 2.23 g (3.12 mmol, 80 %) **[Compound-I]**
- **b.** X=L; Y=L; Z=L: 4.71 g (6.59 mmol, 80 %) **[Compound-II]**

Synthesis of 16-Hydroxypalmitic acid-(W)-Phe-(X)-Phe-(Y)-Phe-(Z)-Phe-OH: Molecule-VI (3.27 gm, 3.73 mmol) was dissolved in calculated amount of methanol ***(***20 ml***)*** and NaOH ***(***2M NaOH***:*** 14 ml***)*** was added dropwise to the solution**.** The progress of the reaction was monitored by TLC**.** After completion of the reaction, as determined by TLC, the methanol was evaporated**.** The residue containing the sodium salt was dissolved in water and extracted with diethyl ether to remove the unreacted stuff**.** The aqueous layer obtained was cooled, acidified with 2N HCl and extracted with ethyl acetate**.** The solvent was evaporated *in vacuo* to obtain a white solid**.**

Yield: 16-Hydroxypalmitic acid-**(**W**)**-Phe-**(**X**)**-Phe-**(**Y**)**-Phe-**(**Z**)**-Phe-OH

- **a.** W=D; X=D; Y=D; Z=D: 2.73 g (3.17 mmol, 85 %) **[Compound-III]**

Synthesis of 16-Hydroxypalmitic acid-(Y)-Phe-(Z)-Phe-OH: Molecule-V (3.26 gm, 5.61 mmol) was dissolved in calculated amount of methanol ***(***20 ml***)*** and NaOH ***(***2M NaOH***:*** 14 ml***)*** was added dropwise to the solution**.** The progress of the reaction was monitored by TLC**.** After completion of the reaction, as determined by TLC, the methanol was evaporated**.** The residue containing the sodium salt was dissolved in water and extracted with diethyl ether to remove the unreacted stuff**.** The aqueous layer obtained was cooled, acidified with 2N HCl and extracted with ethyl acetate**.** The solvent was evaporated *in vacuo* to obtain a white solid**.**

Yield: 16-Hydroxypalmitic acid-(Y)-Phe-(Z)-Phe-OH

a. Y=D; Z=D: 2.54 g (4.48 mmol, 80 %) **[Compound-IV]**

Synthesis of Boc-(X)-Phe-(Y)-Phe-(Z)-Phe-OH: Molecule-III (3.0 gm, 5.22 mmol) was dissolved in calculated amount of methanol (20 ml) and NaOH (2M NaOH: 14 ml) was added dropwise to the solution. The progress of the reaction was monitored by TLC. After completion of the reaction, as determined by TLC, the methanol was evaporated. The residue containing the sodium salt was dissolved in water and extracted with diethyl ether to remove the unreacted stuff. The aqueous layer obtained was cooled, acidified with 2N HCl and extracted with ethyl acetate. The solvent was evaporated *in vacuo* to obtain a white solid.

Yield: Boc-(X)-Phe-(Y)-Phe-(Z)-Phe-OH

a. X=D; Y=D; Z=D: 2.3 g (4.10 mmol, 80 %) **[Compound-V]**

Compound-I:(16 HPA-D-Phe-D-Phe-D-Phe-OH): Yield: 2.23 gm (80%); **IR (cm^{-1}):** 3289, 2914, 2850, 1705, 1672, 1640, 1512, 1248; **LC-MS:** $C_{43}H_{59}N_3O_6$: (OBTAINED) m/z - 712 $[M - H]^+$; MS (calculated) m/z – 713 $[M]^+$; **^{1}H NMR** (500 MHz; d_6-DMSO; in ppm): 8.29 (Phe(3)NH, 1H, *d*, *J* =10Hz); 7.98 (Phe(2)NH, 1H, *d*, *J* =10Hz); 7.89 (Phe(1)NH, 1H, *d*, *J* =10Hz); 7.26 -7.19 (15H, *m*, aromatic H's of Phe(1),(2)&(3)); 4.58 - 4.53 (C$^\alpha$Hs of Phe(3), 1H, *m*); 4.49 - 4.46 (C$^\alpha$Hs of Phe(2), 1H, *m*); 4.35-4.31 (C$^\alpha$Hs of Phe(1), 1H, *m*);4.04-3.93 (Hydroxy Hs of 16-HPA, 1H, *b*); 3.11-2.60 (C$^\beta$H$_s$ of (Phe(3), 2H, *m*); 2.21-2.15 (C$^\beta$H$_s$ of Phe(2) & (1), 4H, *m*); 1.97-1.92 (Methylene adjacent to CO of 16-HPA, 2H, *m*); 1.25-1.23 (Methylene Hs of 16-HPA, 26H, *m*);

Compound-II(16 HPA-L-Phe-L-Phe-L-Phe-OH): Yield: 4.71 gm (80%); **IR (cm^{-1}):** 3192, 3028, 1658, 1459, 1336; **LC-MS:** $C_{43}H_{59}N_3O_6$: (OBTAINED) m/z - 714 $[M + H]^+$; MS (calculated) m/z – 713 $[M]^+$; **^{1}H NMR** (500 MHz; d_6-DMSO; in ppm): 8.46 (Phe(3)NH, 1H, *d*, *J* =10Hz); 8.30 (Phe(2)NH, 1H, *d*, *J* =10Hz); 7.88 (Phe(1)NH, 1H, *d*, *J* =10Hz); 7.23 -7.11 (15H, *m*, aromatic H's of Phe(1),(2)&(3)); 4.59 - 4.53 (C$^\alpha$Hs of Phe(3), 1H, *m*); 4.49 - 4.45 (C$^\alpha$Hs of Phe(2) & Phe (1), 2H, *m*); 4.32 (Hydroxy Hs of 16-HPA, 1H, *b*); 3.12-3.02 (C$^\beta$H$_s$ of (Phe(3), 2H, *m*); 2.94-2.84 (C$^\beta$H$_s$ of Phe(2), 2H, *m*);); 2.76-2.66 (C$^\beta$H$_s$ of Phe(1), 2H, *m*); 1.97-1.94 (Methylene adjacent to CO of 16-HPA, 2H, *m*); 1.42-1.22 (Methylene Hs of 16-HPA, 26H, *m*);

Compound-III:(16 HPA-D-Phe-D-Phe-D-Phe- D-Phe-OH): Yield: 2.73 gm (85%); **IR (cm^{-1}):** 3276, 2915, 2849, 1709, 1636, 1540, 1242; **LC-MS:** $C_{52}H_{68}N_4O_7$: (OBTAINED) m/z - 862 $[M + H]^+$; MS (calculated) m/z – 861 $[M]^+$; **^{1}H NMR** (500 MHz; d_6-DMSO; in ppm): 8.32 (Phe(4)NH, 1H, d, *J* =10Hz); 8.10 (Phe(3)NH, 1H, d, *J* =10Hz); 7.92-7.89 (Phe(1) & (2)NH, 2H, *m*); 7.31-7.08 (Aromatic Hs of Phe(1), (2), (3) & (4), 20H, *m*); 4.61 - 4.55 (C$^\alpha$Hs of Phe(4), 1H, *m*); 4.51 - 4.42 (C$^\alpha$Hs of Phe(3) & (2), 2H, *m*); 4.35 - 4.29 (C$^\alpha$Hs of Phe(1), 1H, *m*); 4.01 – 3.91 (Hydroxy Hs of 16-HPA, 1H, *b*); 3.12 – 2.67 (C$^\beta$H$_s$ of Phe(1), (2), (3) & (4), 8H, *m*); 2.0 – 1.88 (Methylene adjacent to CO of 16-HPA, 2H, *m*); 1.26-

1.22 **(**Methylene Hs of 16-HPA, 28H, *m***)**; 1.16-1.14 **(**Methylene adjacent to OH of 16-HPA, 1H, *b***)**; 1.05-1.00 **(**Methylene adjacent to OH of 16-HPA, 1H, *b***)**

Compound-IV:(16 HPA-D-Phe-D-Phe-OH): Yield: 2.54 gm (80%); **IR (cm^{-1}):** 3260, 2918, 2850, 1767, 1710, 1519, 1641, 1215; **LC-MS:** $C_{34}H_{50}N_2O_5$: (OBTAINED) m/z - 567.4 $[M + H]^+$; MS (calculated) m/z – 566 $[M]^+$**; ^{1}H NMR (**500 MHz; d_6-DMSO; in ppm**):** 8.19 **(**Phe**(**2**)**NH, 1H, *d*, *J* =10Hz **)**; 7.94 **(**Phe**(**1**)**NH, 1H, *d*, *J* =10Hz **)**; 7.29 -7.15 **(**10H, *m*, aromatic H**'**s of Phe**(**1**),(**2**)&(**3**))**; 4.59 - 4.51 **(**C^{α}Hs of Phe**(**2**)**, 1H, *m***)**; 4.48 - 4.41 **(**C^{α}Hs of Phe**(**1**)** 1H, *m***)**; 4.30-4.23 **(**Hydroxy Hs of 16-HPA, 1H, *m***)**; 3.11-3.05 **(**$C^{\beta}H_s$ of **(**Phe**(**2**)**, 1H, *m***)**; 3.02-2.96 **(**$C^{\beta}H_s$ of Phe**(**2**)**, 1H, *m***)**; **)**; 2.74-2.65 **(**$C^{\beta}H_s$ of Phe**(**1**)**, 2H, *m***)**; 2.00-1.95 **(**Methylene adjacent to CO of 16-HPA, 2H, *m***)**; 1.44-1.01 **(**Methylene Hs of 16-HPA, 26H, *m***)**;

Compound-V:(Boc-D-Phe-D-Phe-D-Phe-OH): Yield: 2.3 gm (80%); **IR (cm^{-1}):** 3277, 2917, 2852, 1637, 1531; **LC-MS:** $C_{32}H_{37}N_3O_6$: (OBTAINED) m/z - 559.8 $[M]^+$; MS (calculated) m/z – 559 $[M]^+$**; ^{1}H NMR (**500 MHz; d_6-DMSO; in ppm**):** 8.29 **(**Phe**(**3**)**NH, 1H, *d*, *J* =10Hz **)**; 7.97 **(**Phe**(**2**)**NH, 1H, *d*, *J* =10Hz **)**; 7.89 **(**Phe**(**1**)**NH, 1H, *d*, *J* =10Hz **)**; 7.23-7.18 **(**Aromatic Hs of Phe**(**1**),(**2**)&(**3**)**, 15H, *m***)**; 4.56 - 4.31 **(**C^{α}Hs of Phe**(**1**)**, **(**2**)** & **(**3**)**, 3H, *m***)**; 3.10-2.60 **(**$C^{\beta}H_s$ of **(**Phe**(**1**)**, **(**2**)** & **(**3**)**, 6H, *m***)**; 1.24 **(**Methyl Hs of Boc, 9H, *s***)**

Protocols for Various Analysis

1. **DFT Calculations:** The molecules were created using Spartan08 software package and structure optimizations were done using a molecule of hydrogelator in Gaussian09.[1,2] B3LYP method was used along with 6-31G basis set. Optimization and frequency calculations were done using tight convergence criteria and all the negative frequencies were removed to get the structure at its minimum potential energy. Partition coefficients were calculated by optimizing the structures in water and n-octanol as solvent using CPCM model in Gaussian09. The solvation energies obtained from minimizations with all positive frequencies were considered. The partition coefficient was calculated using the formula:

   $\log P = \frac{-\Delta G_{n-octanol/water}}{RTln10}$ where, $\Delta G°_{\text{n-octanol/water}} = \Delta G°_{\text{n-octanol}} - \Delta G°_{\text{water}}$

2. **Preparation of Gels:** Required quantity of Compounds **(I-V)** were separately dissolved in 9.2 pH phosphate buffer and gently warmed until a clear solution was formed. Compounds were left undisturbed for some time until the solvent was immobilized, and the formation of gels was confirmed by the inverted test tube method.
3. **MTT Assay:**

   Materials

   Dulbecco`s Modified Eagle Media (DMEM) with low glucose -Cat No-11965-092 (Gibco, Invitrogen) Fetal bovine serum (FBS) - Cat No -10270106 (Gibco, Invitrogen)

   Antibiotic – Antimycotic 100X solution (Thermofisher Scientific)-Cat No-15240062

Negative Control- Untreated Cells with media

Cytotoxicity Protocol-

The cells were seeded in a 96-well flat-bottom microplate and maintained at 37ºC in 95% humidity and 5% CO_2 overnight. Different concentration (100, 50, 25, 12.5, 6.25, and 3.125 µg/ml) of samples were treated. The cells were incubated for another 48 hours. The wells were washed twice with PBS and 20 µL of the MTT staining solution was added to each well and the plate was incubated at 37°C. After 4h, 100 µL of DMSO was added to each well to dissolve the formazan crystals, and absorbance was recorded with a 570 nm using microplate reader (1).

Formula:

Surviving cells (%) = Mean OD of test compound /Mean OD of Negative control ×100

4. Docking studies

The atomic coordinates of receptor MCT1 with PDB ID: 1PW4 was downloaded from the Protein Data Bank. To gain a better understanding, standard drug (Capecitabine) and Compounds I-V were docked using the same constraints at the active site. The structures were imported into the Maestro module (v9.3) available in the Schrödinger Trial package and the protein was optimized using the Protein Preparation Wizard

5. Detailed Anti-Cancer Activities

5.1 ROS Estimation with Flow Cytometry- MCF-7

MCF-7 cells were plated in 6 well plates at a density of 5000 to 10000 cells/well in 1ml DMEM medium supplemented with 10% FBS and 1% Antibiotic solution, and incubated for 24 h at 37**°C &** 5% CO_2. Cells without Treatment were considered as Control. After incubation, old medium was removed and fresh culture medium was added before treatment. Then cells were treated at different concentrations (mentioned in Excel sheet) and further incubated for 24 h. After incubation, medium was removed and add cells were harvested with trypsin EDTA and collected in 1.5 ml tube and washed once with 500µl chilled PBS. Finally, cells pellet was dispensed in 100 µl PBS with 2µM DCFDA and acquired the samples in Flow Cytometer ((BD FACS Calibur, USA) within 1 hour. Acquired data were analyzed by using flowing software version 2.5.1

5.2 Cell Proliferation Assay: Cell Proliferation on MCF-7 cell line was determined by Alamar blue assay. The cells (5000-8000 cells/well) were cultured in 96 well plate for 24 h in DMEM medium supplemented with 10% FBS and 1% antibiotic solution at 37°C with 5% CO_2. Cells were treated at different concentration of treatment doses for 24 hours. 10 µl of Alamar Blue reagent per 100 µl medium was added after 24 hours and further incubated for 3-4 h. Finally, the plate was read at 540/590nm using fluorescence ELISA Plate reader (Agilent BioTek Epoch 2)

5.3 DNA Fragmentation Analysis: The MCF-7 cells **(**10000 cells/well**)** were cultured in 96 well plate for 24 h in DMEM **(**Dulbecco's Modified Eagle MediumAT149-1L**)** medium supplemented with 10**%** FBS **(**Fetal Bovine Serum **-** HIMEDIA-RM 10432**)** and 1**%** antibiotic

solution at 37°C with 5**%** CO_2**.** Next day cells were treated from IC_{50} dosage of the formulations and incubated for 24 hours**.** After 24 hours, dead cells were collected, and DNA was isolated with standard protocol of DNA Isolation**.** The sample was characterized with 1**%** agarose gel electrophoresis for 30 minutes at 90V and image captured in gel documentation system **(**CAMAG**-** Repostar 3 equipped with Canon 1300D**)**

5.4 Gene Expression Analysis with Conventional PCR

Cell line was purchased from NCCS Pune. The cells (8-10,000 cells/well) were cultured in 96 well plate in DMEM (HIMEDIA- AT149-1L) medium supplemented with 10% FBS (HIMEDIA-RM 10432-500M) and 1% antibiotic solution at 37°C with 5% CO2. Cells after 12-24 hours seeding were treated with effective dose for 24 hours, and RNA isolation step was followed. RNA isolation from cells (samples were pooled from 8 wells of 96 well plate) was performed by using Trizol (Thermo Scientific) by following the manufacturer's protocol. The integrity of isolated RNA was checked on agarose gel (1.5% w/v). Preparation of cDNA was done by using PrimeScript™ 1st strand cDNA Synthesis Kit by following the manufacturer's protocol. 2 microgram total RNA along with the equal amount of random hexamers and oligo dT primers were used for synthesis of cDNA. Genes were amplified by PCR (T100 Thermocycler, Biorad, USA). PCR product was analyzed in 2% agarose gel electrophoresis. Gel was run for 30 mins at 90V. Gel images were captured in gel documentation system and densitometric analysis was carried out using ImageJ software, (from NCBI). Data were normalized with the GAPDH expression.

5.5 Protein Expression Analysis – EL – TNF - α

Experiment was performed as per kit instructions (GENLISA™ Human TNF α ELISA- Cat No.: KB1145) 100 µl standard (TNF α- 1 µg/ml) and sample (*IC_{50}* dose) was added to the plate, plate was sealed and incubated for 2 h at room temperature. Cells without treatment were considered as Control. Plate was washed four times with wash buffer (1X) and buffer was blotted by firmly tapping plate upside down on absorbent paper. Diluted detection antibody (Biotin Conjugated Detection Antibody) solution was added 100µl to each well, plate was sealed and incubated for an hour at room temperature. Again, plate was washed with wash buffer (1X) then 100µl diluted Streptavidin -HRP solution was added to each well, plate was sealed and incubated for an hour. Plate was washed with wash buffer (1X) and 100µl TMB substrate (3,3',5,5'-Tetramethylbenzidine) solution was added and incubated in dark for 30 minutes. To stop the reaction, 100 µl of stop solution was added to each well and read the absorbance at 450nm within 30 minutes.

5.6 Protein Expression Analysis with ELISA – IL - 1β

Experiment was performed as per kit instructions (GENLISA^{TM} Human IL-1β ELISA- Cat No.: KB1063) 100 µl standard (IL-1β - 1 µg/ml) and sample was added to the plate, plate was sealed and incubated for 2 h at room temperature. Plate was washed four times with wash buffer (1X) and buffer was blotted by firmly tapping plate upside down on absorbent paper. Diluted detection antibody (Biotin Conjugated Detection Antibody) solution was added 100µl to each well, plate was sealed and incubated for an hour at room temperature. Again, plate was washed with wash buffer (1X) then 100µl diluted Streptavidin -HRP solution was added to each well, plate was sealed and incubated for an hour. Plate was washed with wash buffer (1X) and 100µl TMB substrate (3,3',5,5'-Tetramethylbenzidine) solution was added and incubated in dark for 30 minutes. To stop the reaction, 100 µl of stop solution was added to each well and read the absorbance at 450 nm within 30 minutes.

5.7 Proteolytic and Morphological studies of Compound I

The proteolytic study was carried out by incubating Compound **I** with the proteolytic enzyme proteinase K for 48 h and recording the degradation rate by mass spectrometry, if any at regular intervals of time of 12 h, till 48 hrs.

The Morphological Study before and after proteolysis of Compound **I**, was probed by Field-emission scanning electron microscopy (FE-SEM) experiment on a JEOLscanning electron microscope (model no. JSM-7600F) with xerogels, obtained from the hydrogels of the concentration (25 mg/mL)

5.8 Determination of Conformation of Compound I

The conformation of the Compound **I**, was determined using the following techniques described below with concentration 25 mg/ml for all the structural experiments:

a) **Variable temperature ^{1}H NMR**: Here the sample was analysed using 500 MHz Bruker Advance Instrument with d6-DMSO as a solvent, and the temperature range worked upon was 298K to 333K.
b) **Fourier Transform-Infrared spectroscopy**: This spectrum was recorded using a KBr pellet on an Agilent CARY 620 FTIR spectrophotometer. The background was collected using a blank KBr pellet
c) **PXRD**: Powder X-ray Diffraction (PXRD) Study. The PXRD experiments of the xerogels were carried out using an X-ray diffractometer (Bruker AXS, Model No. D8Advance) operating at 40 kV voltage and 40 mA current. For scanning, the Lynx Eye superspeed detector was used with scan speed 0.3 s and step size 0.028.

5.9 Determination of Rheological Properties of Compound I

Rheological Properties of Compound I, were carried out on an Anton Paar Physica MCR 301 rheometer, where the viscoelastic properties of hydrogels were evaluated as a function of storage modulus (G′) and loss modulus (G″). The requisite amount of hydrogel was transferred on a rheometer plate with a microspatula and kept hydrated using a solvent trap. A stainless steel parallel plate was used to sandwich the hydrogels. The mechanical strengths of the hydrogels were determined by frequency-sweep experiments. The thixotropic nature was investigated by step-strain experiments at the constant frequency of 10 rad/s, and applied strains were varied from 0.1 to 40%

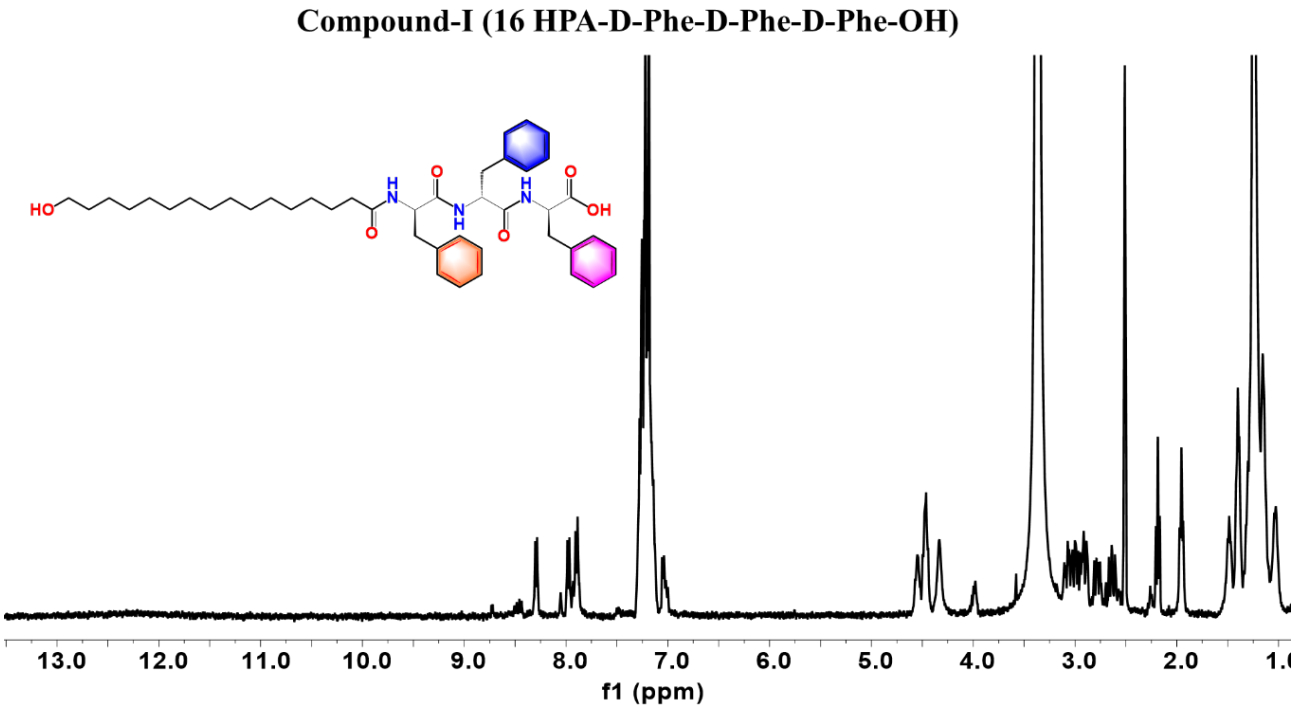

Figure S2A: – ^{1}H-NMR Spectra of Compound **I**

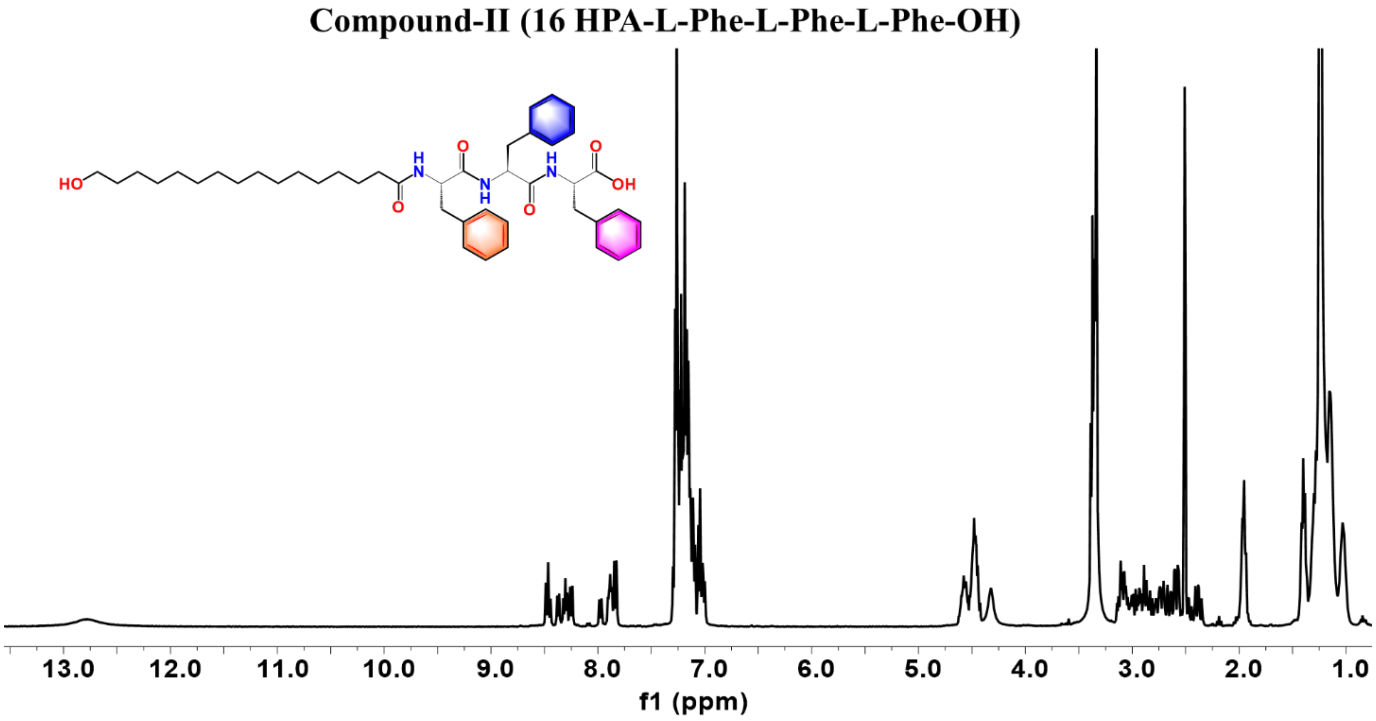

Figure S2B: – ^{1}H-NMR Spectra of Compound **II**

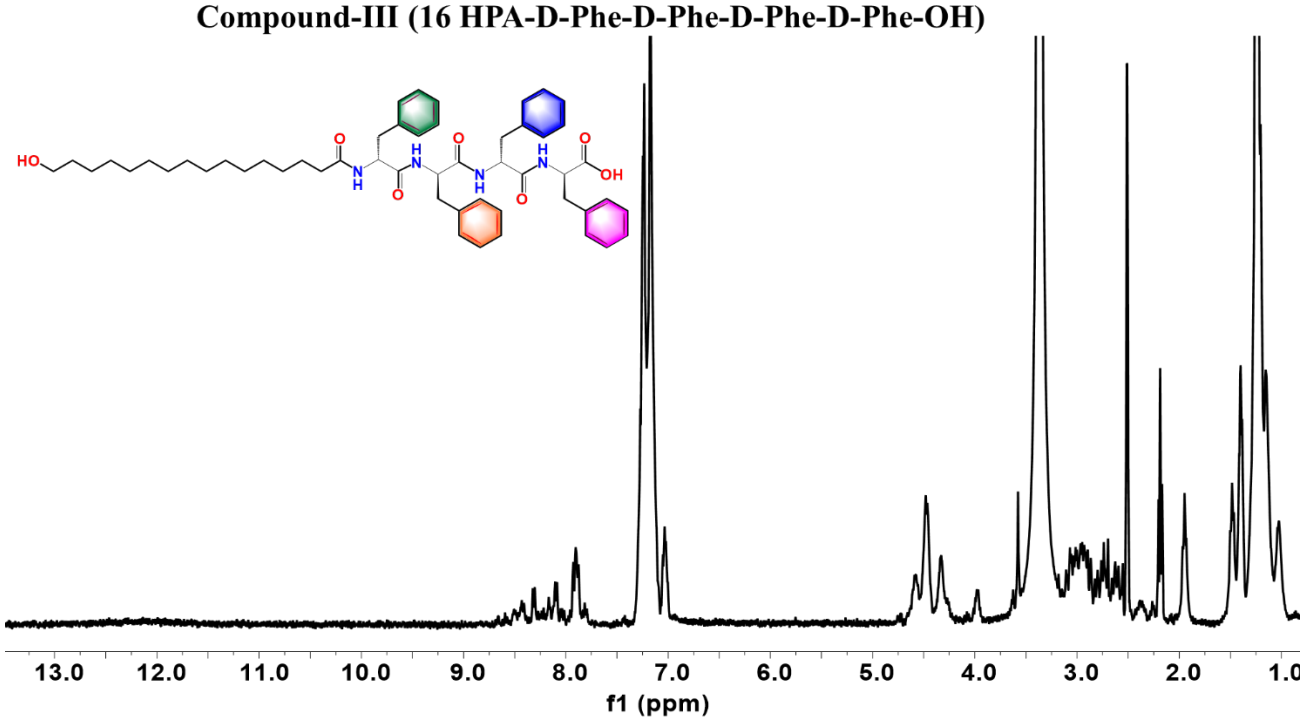

Figure S2C: – ^{1}H NMR Spectra of Compound **III**

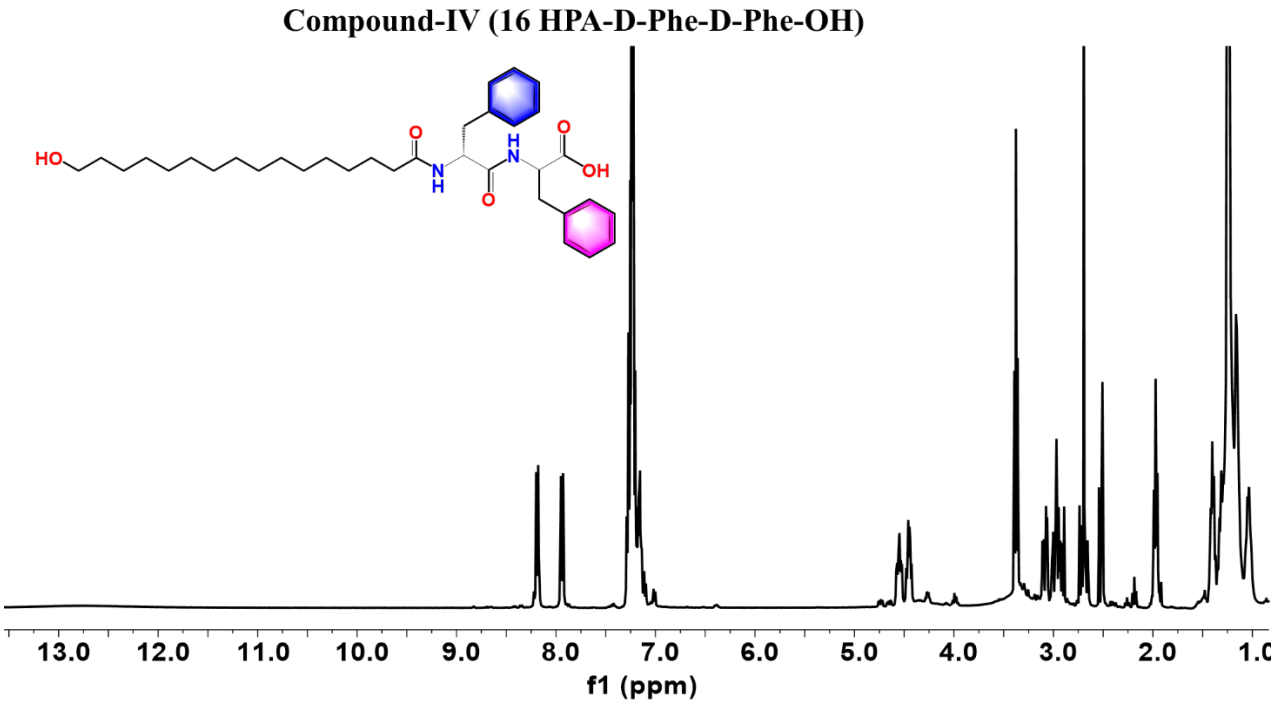

Figure S2D: – ^{1}H NMR Spectra of Compound **IV**

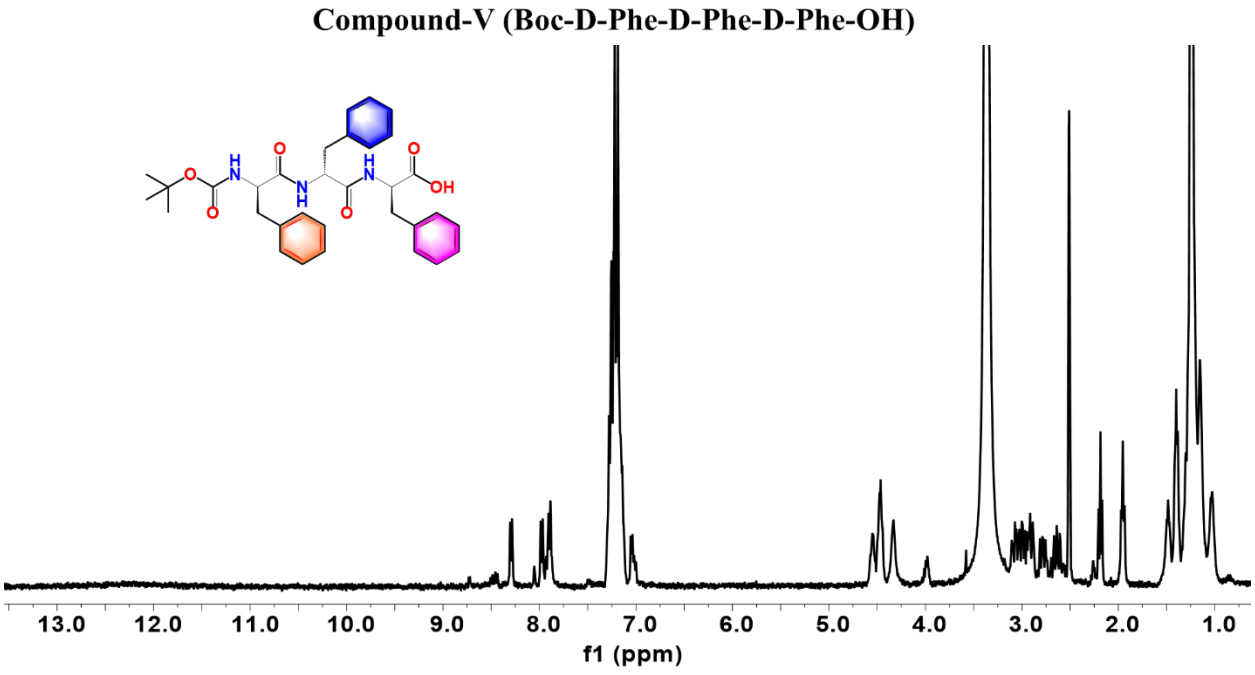

Figure S2E: - ^{1}H NMR Spectra of Compound **V**

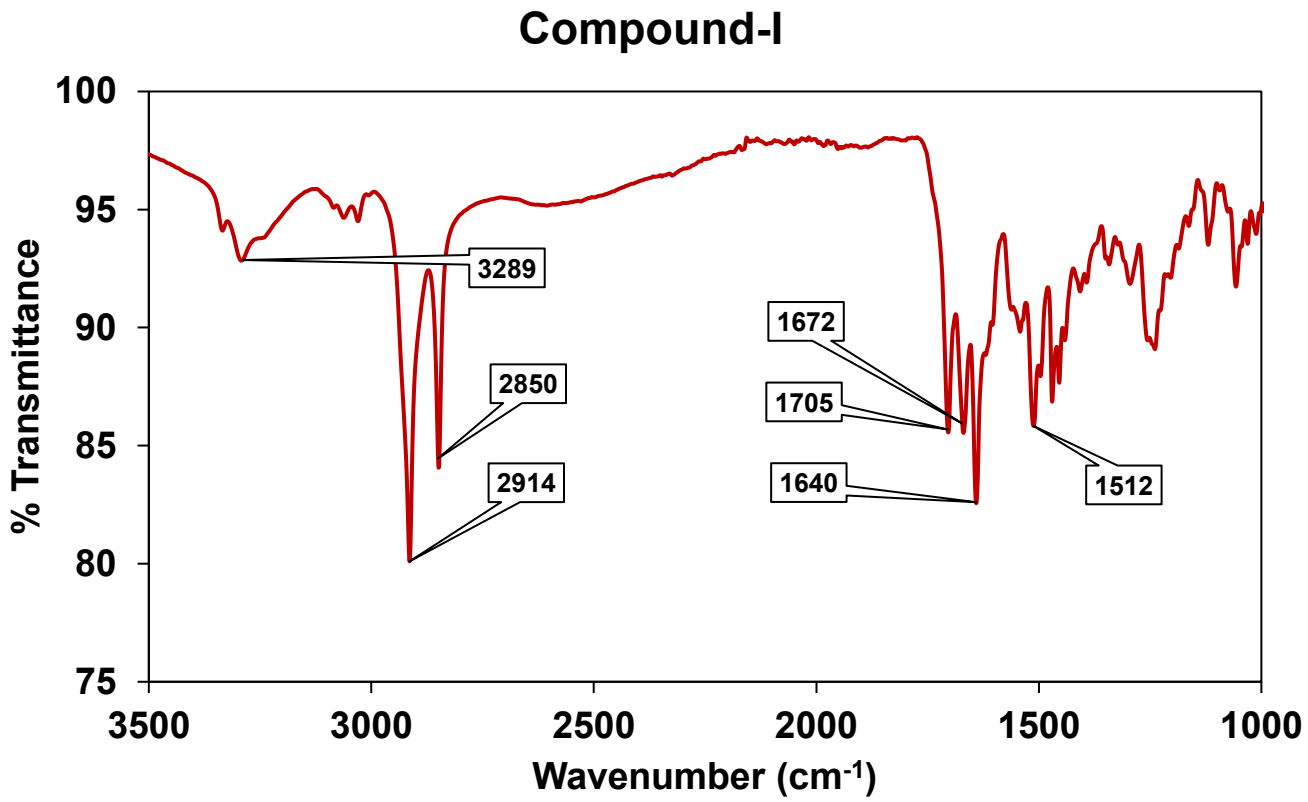

Figure S3A: - FTIR Spectra of Compound **I (solid)**

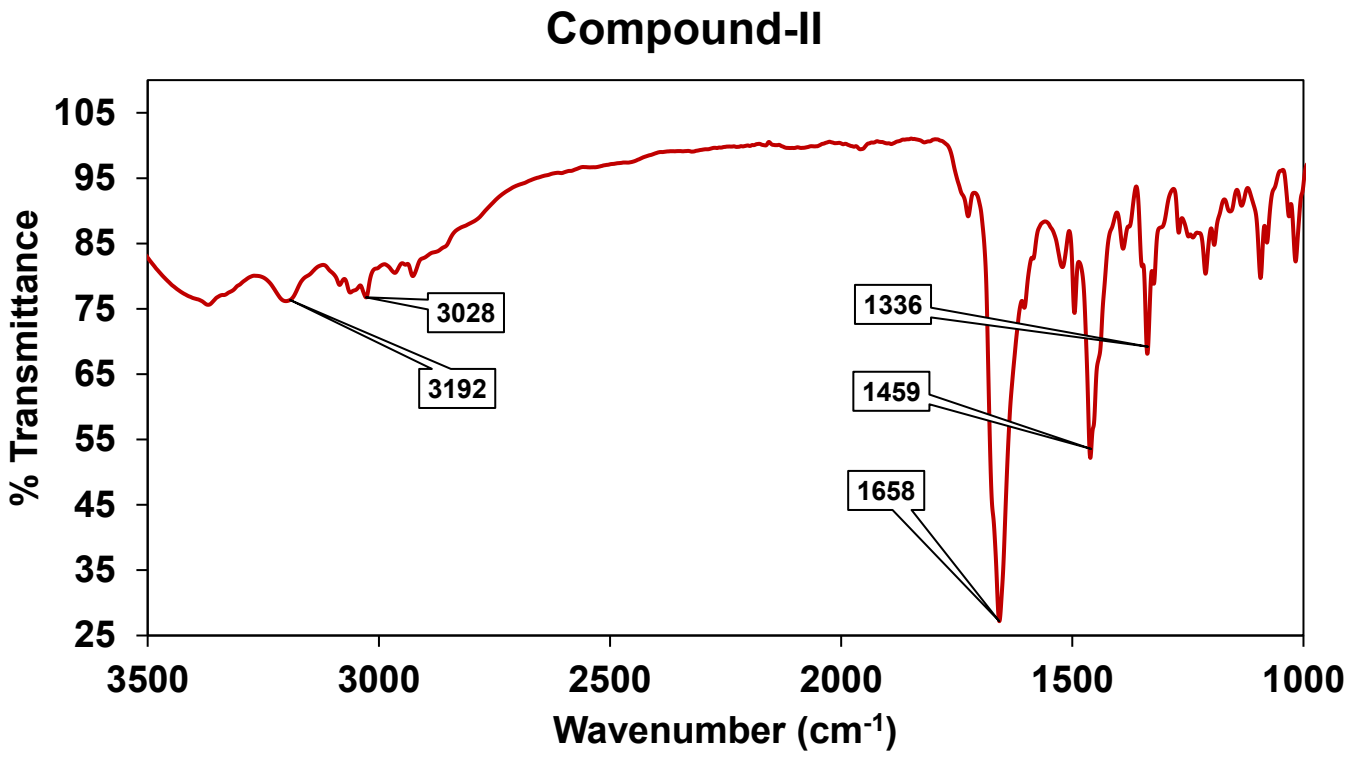

Figure S3B: - FTIR Spectra of Compound **II (solid)**

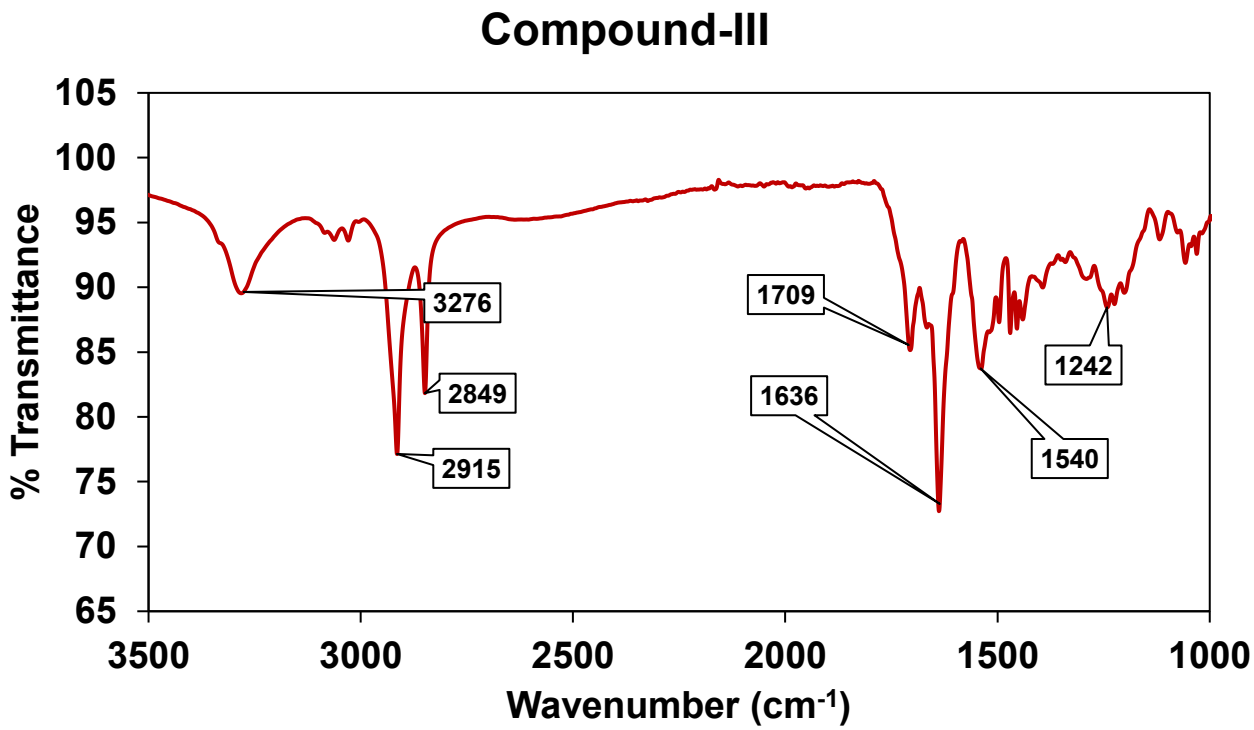

Figure S3C: – FTIR Spectra of Compound **III (solid)**

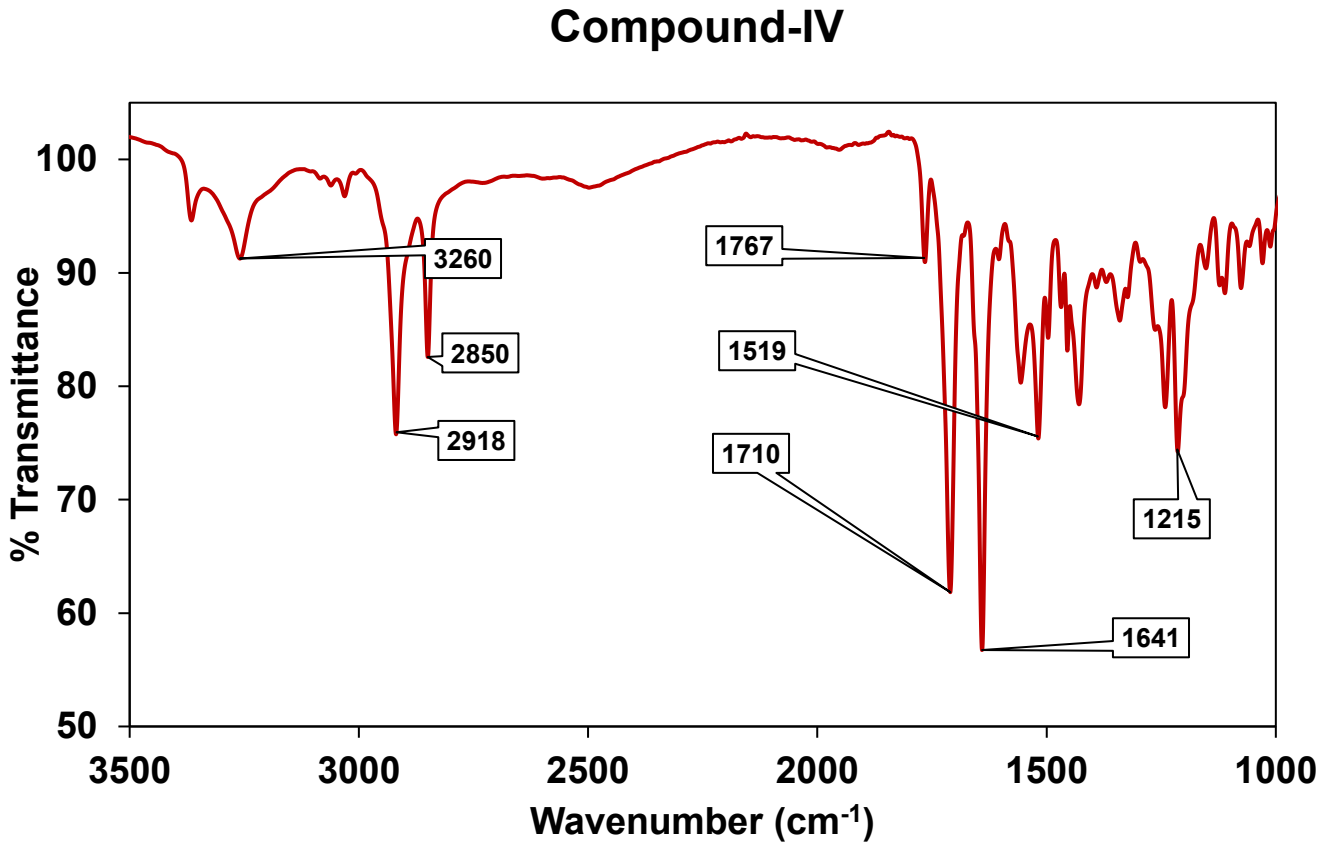

Figure S3D: – FTIR Spectra of Compound **IV (solid)**

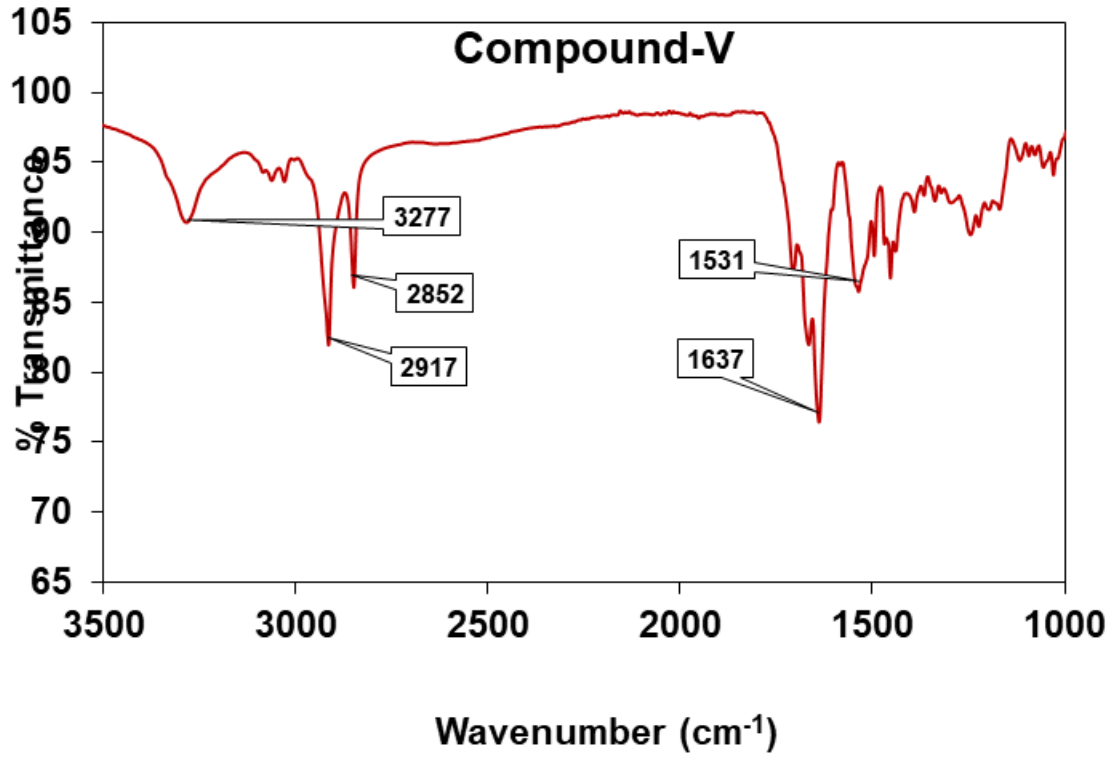

Figure S3E: – FTIR Spectra of Compound **V**

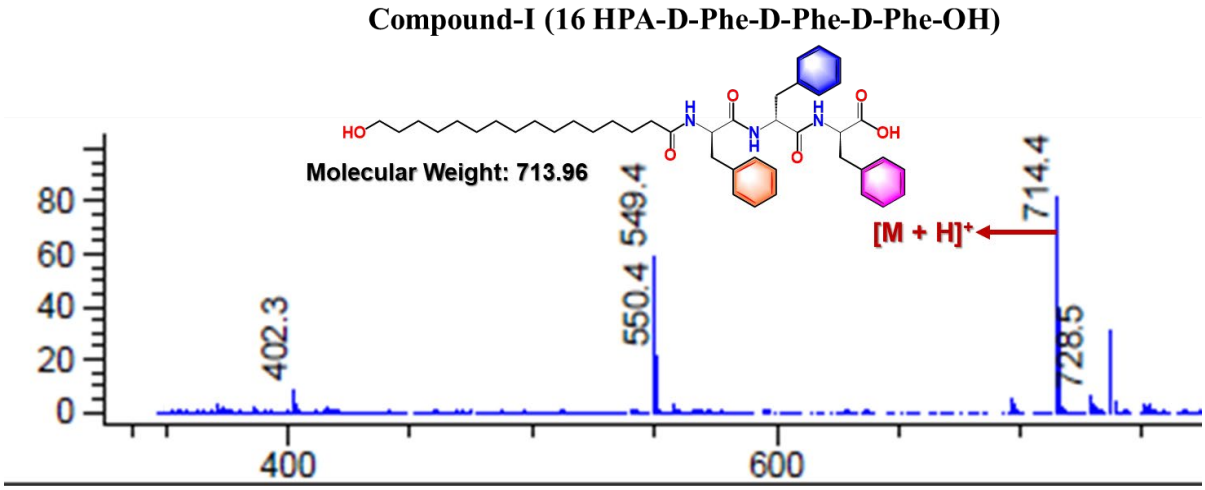

Figure S4A: - Mass Spectra of Compound-**I**

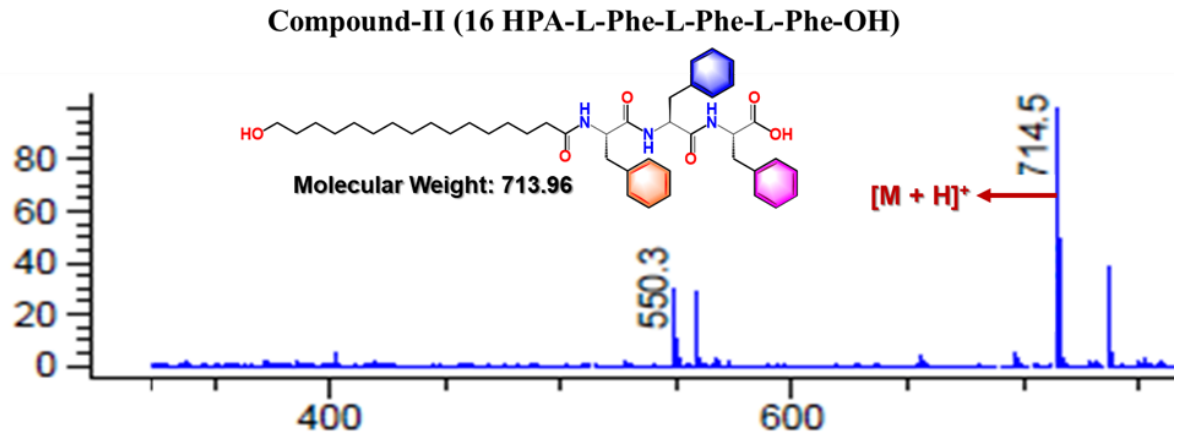

Figure S4B: - Mass Spectra of Compound-**II**

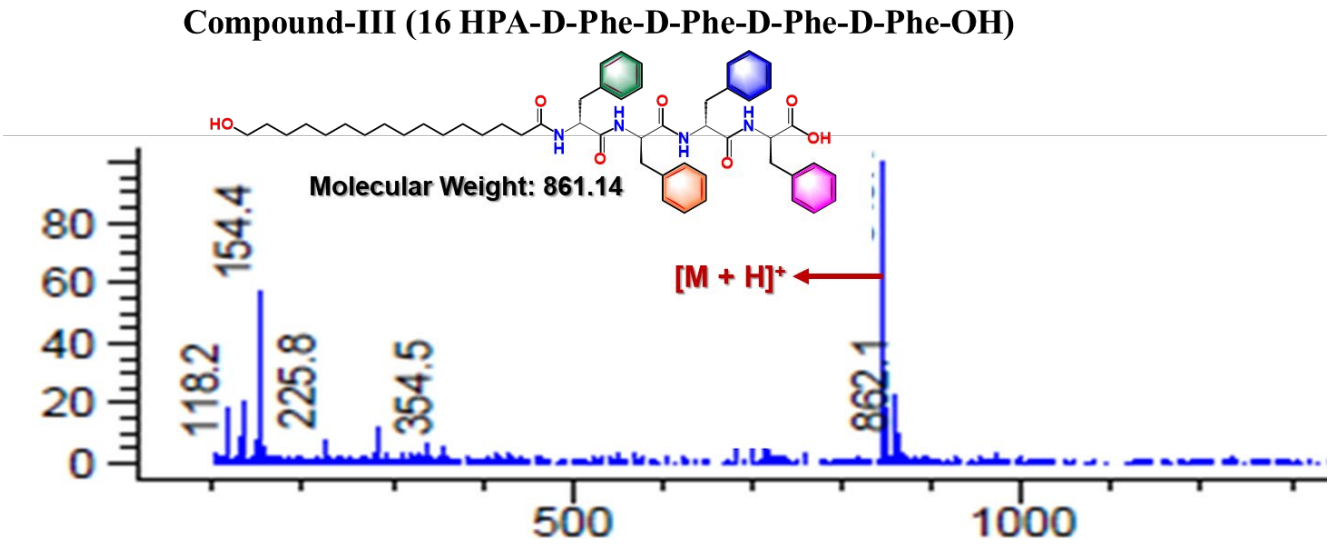

Figure S4C: - Mass Spectra of Compound **III**

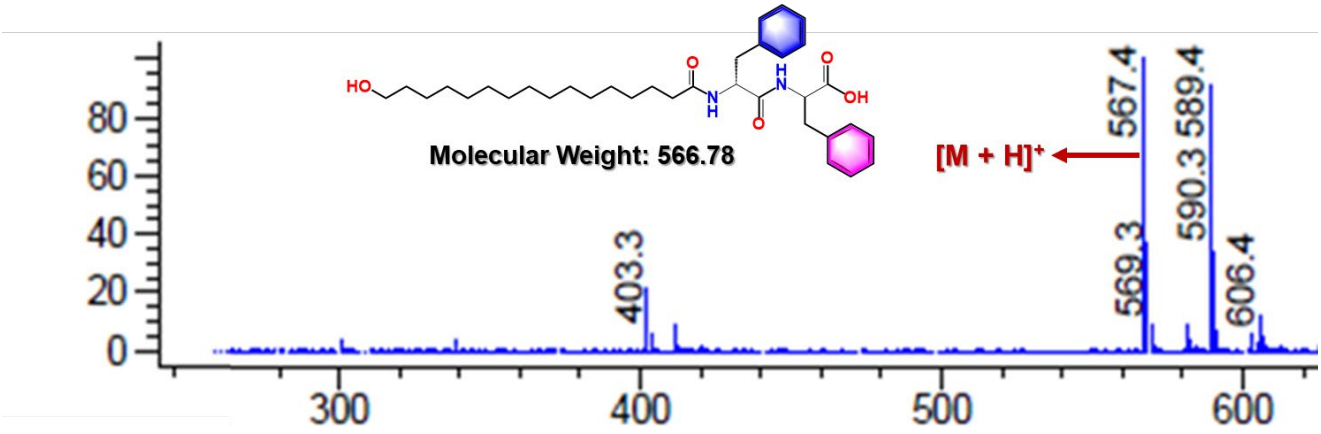

Figure S4D: - Mass Spectra of Compound **IV**

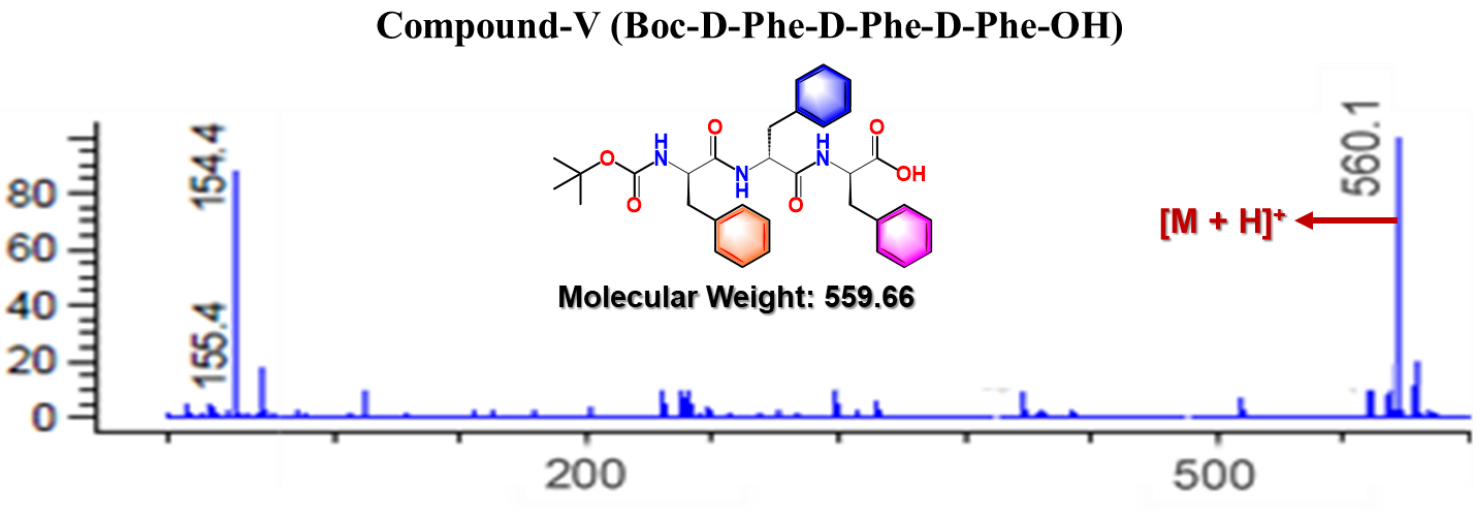

Figure S4E: - Mass Spectra of Compound **V**

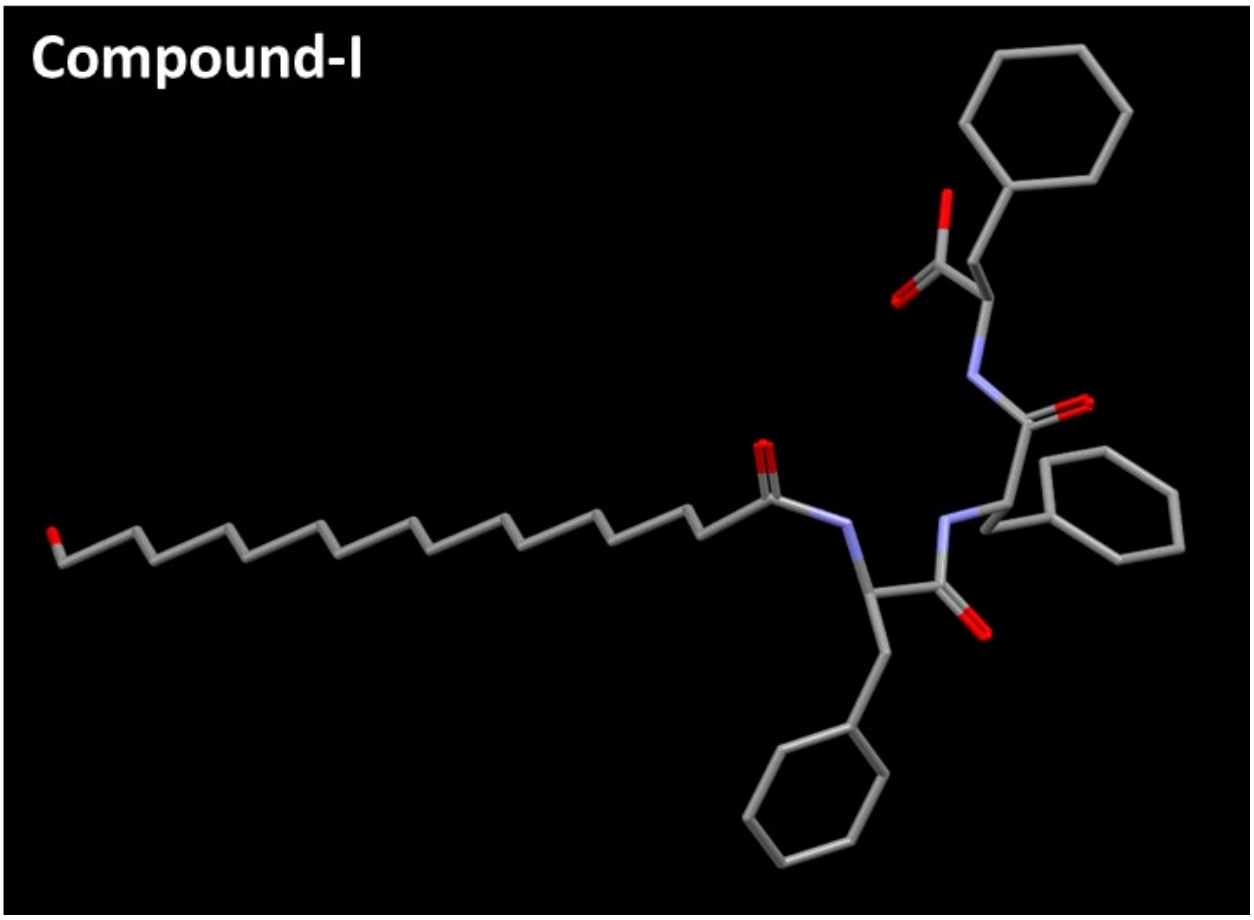

Figure S5A(i): - Energy minimized structure of Compound **I**

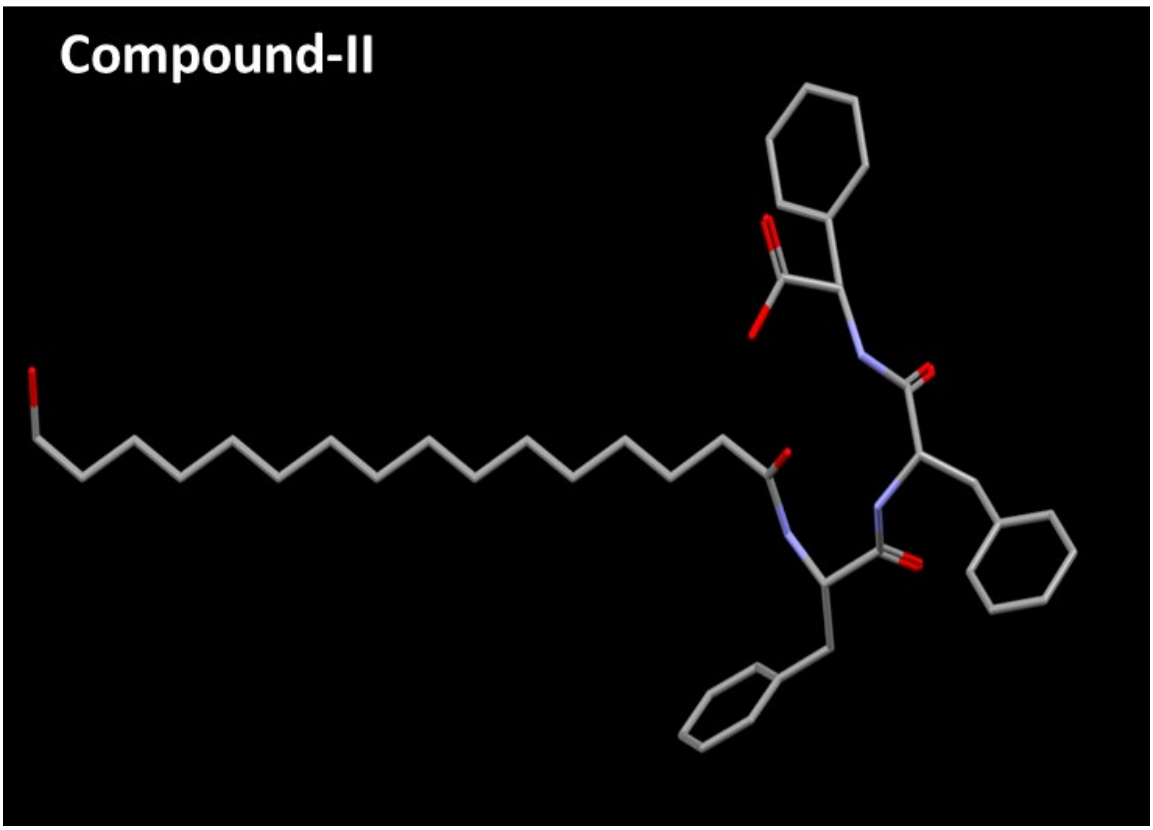

Figure S5A(ii): - Energy minimized structure of Compound **II**

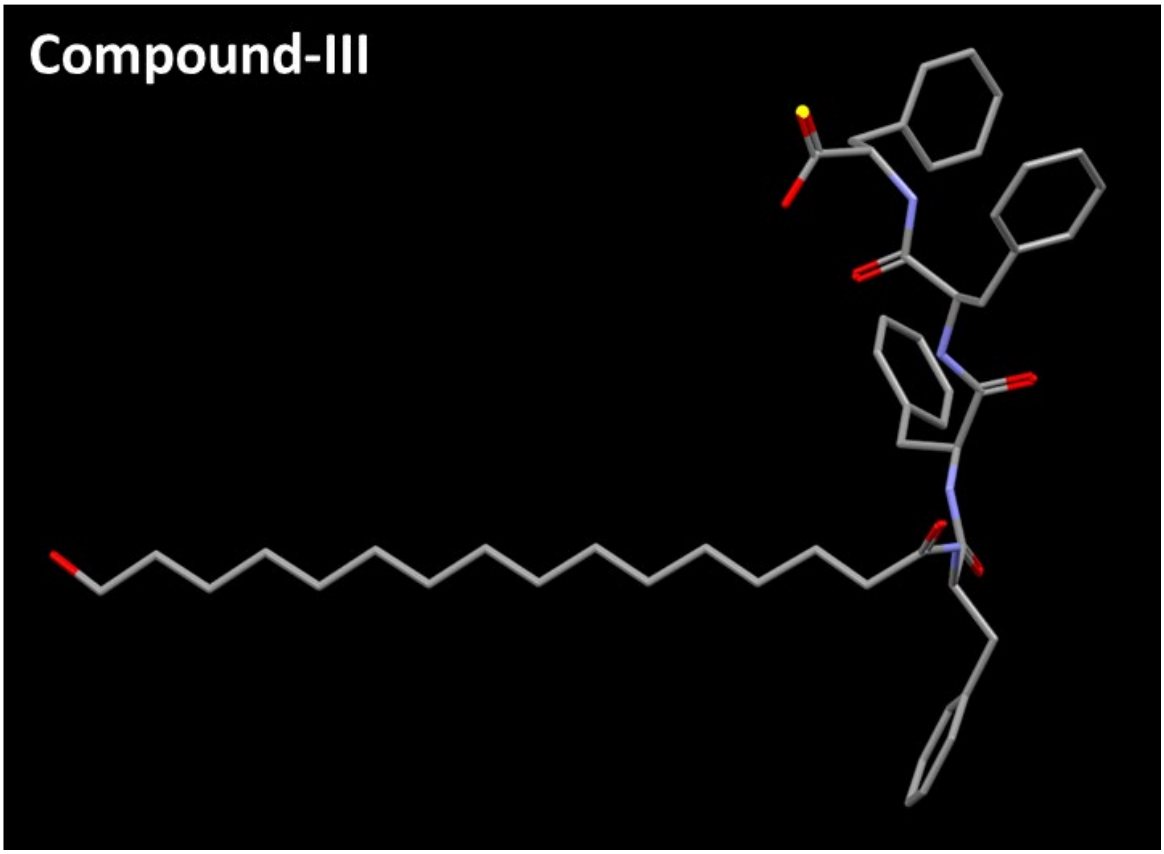

Figure S5A(iii): - Energy minimized structure of Compound **III**

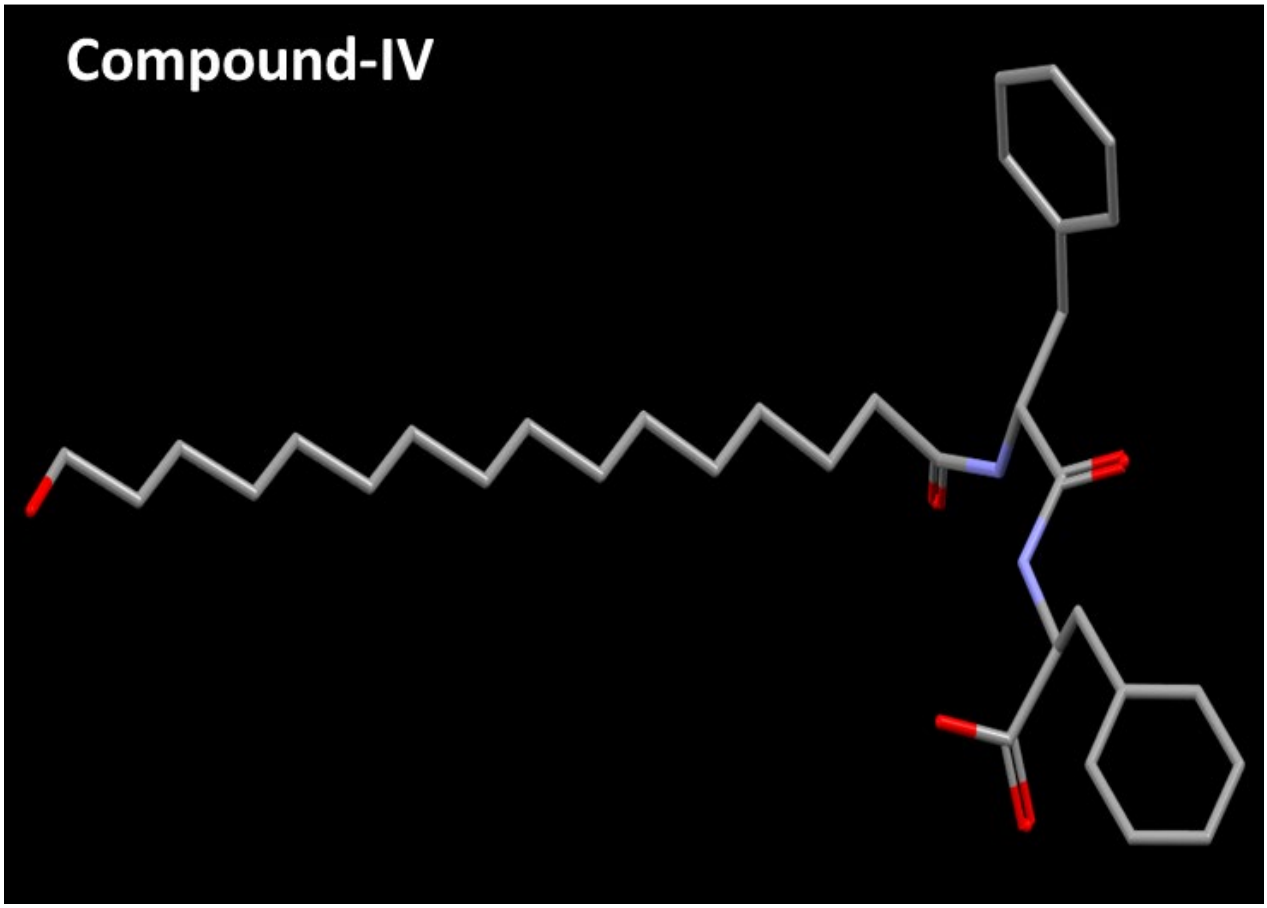

Figure S5A(iv): - Energy minimized structure of Compound **IV**

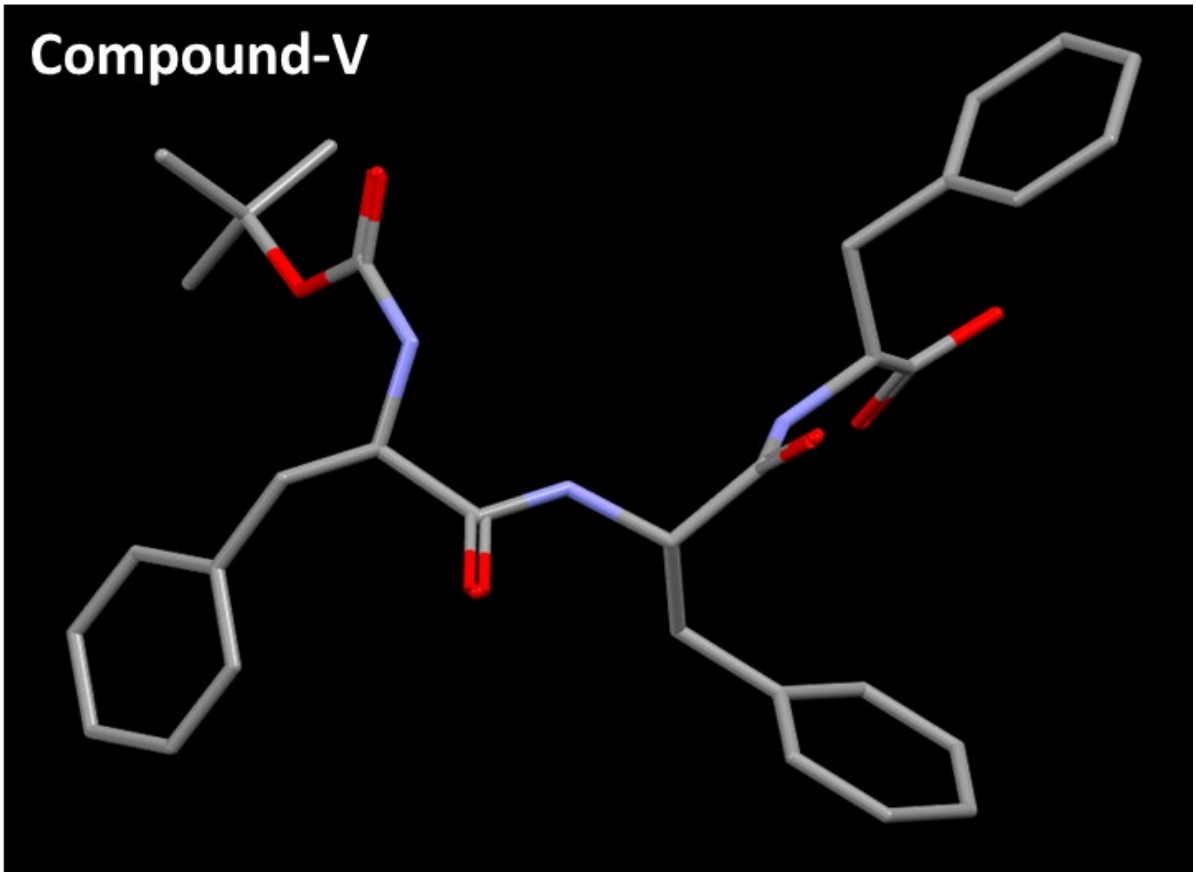

Figure S5A(v): - Energy minimized structure of Compound **V**

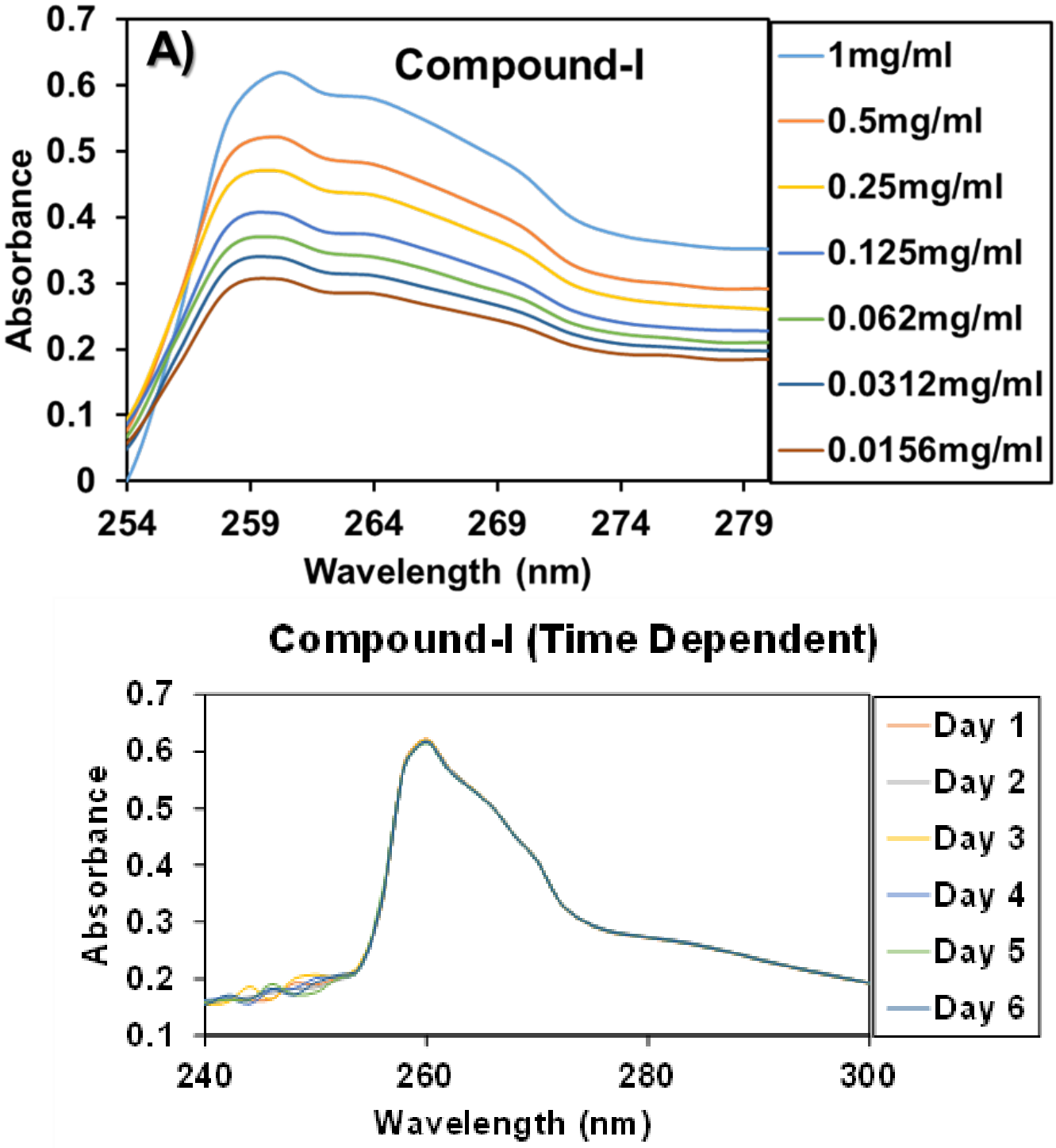

Figure S5B: Stability Studies of Compound-**I**; **(A)** Concentration dependent, **(B)** Time dependent. Studies reveal that there occurs no change in pattern of the spectra even after change of concentration from spectra **A** & Change of Time till Day 6 from Spectra **B**

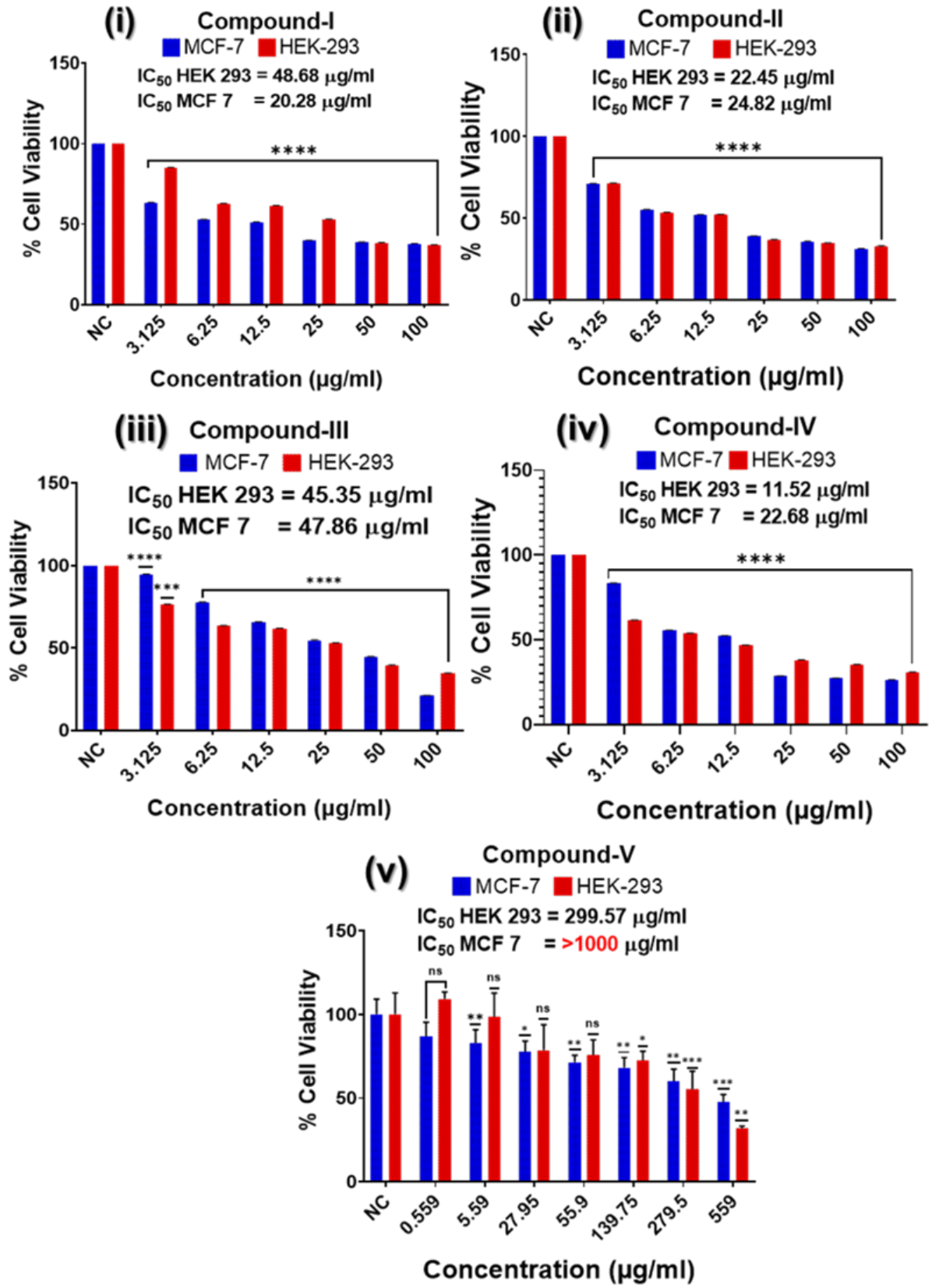

Figure S6 (i-v) Anti-cancer efficacy of Compounds **I - V** screened against two different cell lines namely malignant MCF-7 and noncancerous human embryonic kidney 293T (HEK 293T) by a dose-dependent MTT cell viability assay; Data was statistically analysed using a two-tailed paired Student's t test and presented as mean ± SD (N = 3). ns = not significant, *p<0.05, **<0.01, ***p<0.001 and ****p < 0.0001, as compared to the negative control group.

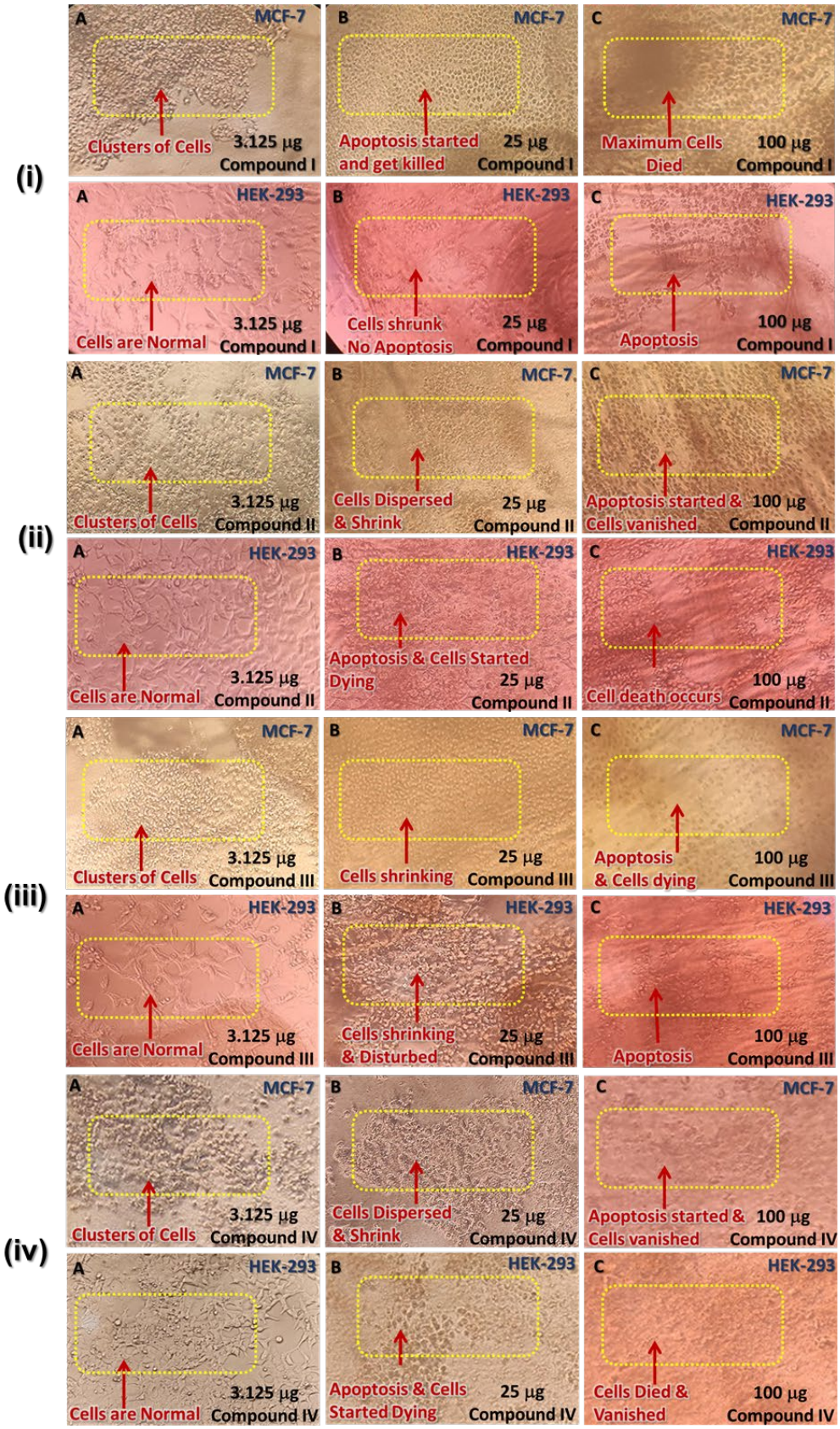

Figure S7 (i-iv) Cellular morphologies of HEK 293 and MCF-7 cancer cell lines after treating with different concentrations of Compounds **I – IV**

Table S1: List of Compounds and their activities reported to prove the anticancer inculcating nature of 16-HPA over others

Serial Number	Molecules	IC_{50} in MCF 7	Ref:
Compound I	16-HPA-D-Phe-D-Phe-D-Phe-OH	20.28 µg/ml Figure S5 (i-v)	This work
Compound II	16-HPA-L-Phe-L-Phe-L-Phe-OH	24.82 µg/ml Figure S5 (i-v)	This work
Compound III	16-HPA-D-Phe-D-Phe-D-Phe-D-Phe-OH	47.86 µg/ml Figure S5 (i-v)	This work
Compound IV	16-HPA-D-Phe-D-Phe-OH	22.68 µg/ml Figure S5 (i-v)	This work
Compound V	Boc-D-Phe-D-Phe-D-Phe-OH	>1000 µg/ml Figure S5 (i-v)	This work

New Compound I	Palmitic acid-D-Phe-D-Phe-D-Phe-OH	>1000 µg/ml	Unpublished work
New Compound II	12-HDA-D-Phe-L-Phe-L-Phe-OH	407 µg/ml	Unpublished work

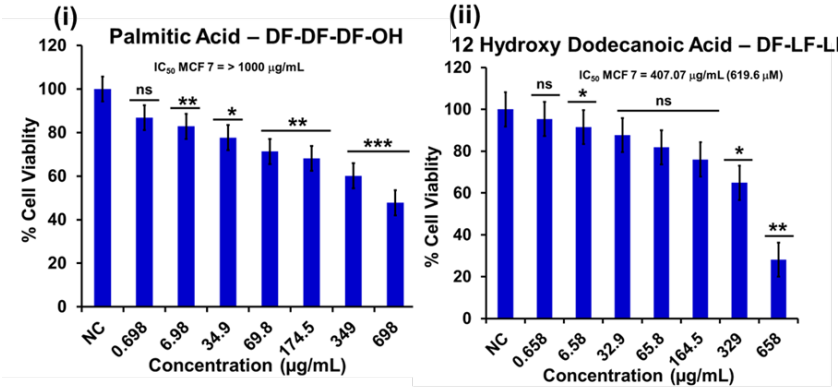

Figure S8. Anti-cancer efficacy of the New Compounds screened against malignant MCF-7 by a dose-dependent MTT cell viability assay; Data was statistically analysed using a two-tailed paired Student's t test and presented as mean ± SD (N = 3). ns = not significant, *p<0.05, **<0.01, ***p<0.001 and ****p < 0.0001, as compared to the negative control group.

Closer look into the values of the IC_{50} in MCF 7 cell lines, indicated that in compounds **I- IV**, tethered to 16-HPA at the N-terminus, irrespective of the number and nature of the chiral residues of phenylalanines, demonstrated higher potency (**Table S1**). However the sooner the amphiphile, 16-HPA was removed, compound **V,** no anticancer activity was observed. Even when the amphiphile palmitic acid was anchored, failed to display necessary activity (**New compound I) (Figure S8, Table S1).** To check the influence of number of methylene units in the amphiphile, we replaced 16-HPA (14 methylenes) by 12-HDA (12 methylenes) and tethered to triphenylalanines of diversified configuration. Here too, we observed almost 10 to 20 times lower activity **New compound II**. Thus the importance of 16-HPA in imparting anticancer activity is emphasized **(Figure S8, Table S1).**

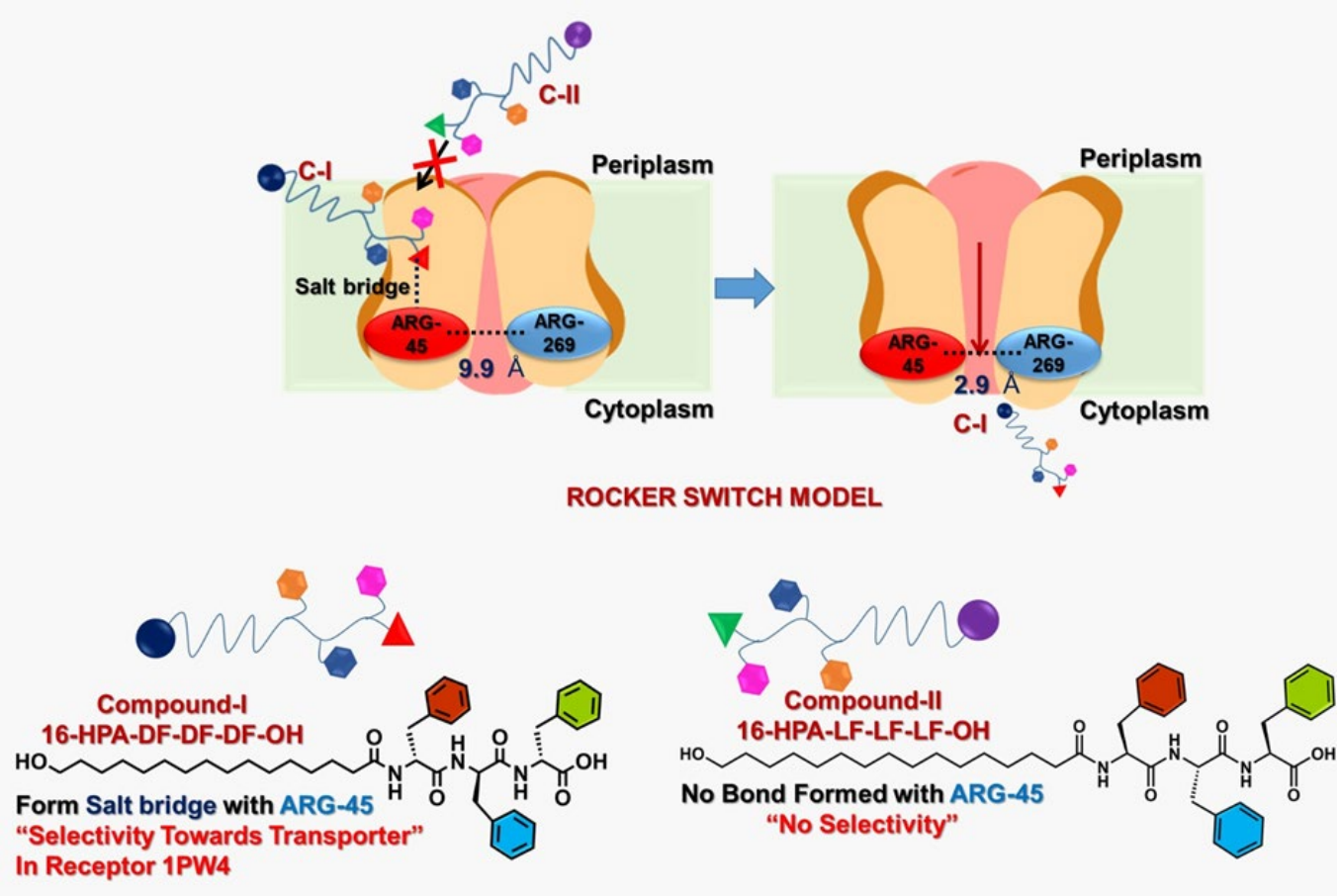

Figure S9: Pictorial representation of Rocker-Switch Model Specify of Compound-**I** with **ARG-45.** We anticipate that appropriate D-D-D chirality in the triphenylalanines in Compound **I**, that might have interacted with Arg 45 leading to salt bridge type correspondence have led to rocker switch type motion, the probable reason for higher selectivity than Compound **II-V,** which lacked appropriate chirality in the chiral amino acid residues and failed to bring them adjacent each other **.**

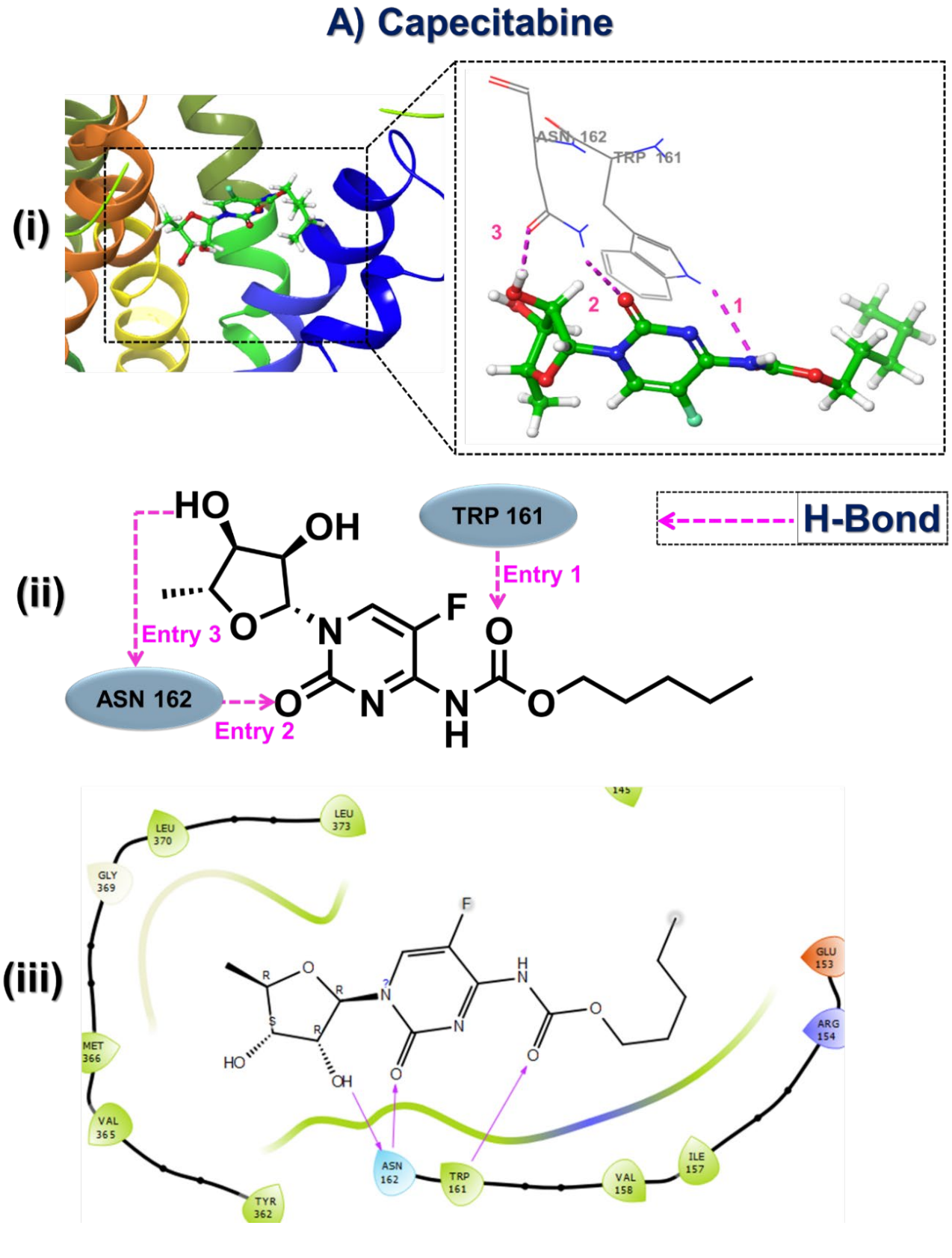

Figure S10:

i) 3D representation of the mode of interactions in Standard Drug - Capecitabine
ii) Pictorial diagram of the mode of interactions in Standard Drug - Capecitabine
iii) 2D representation of the mode of interactions in Standard Drug - Capecitabine

B) 16-HPA-D-Phe-D-Phe-D-Phe-OH (compound-I)

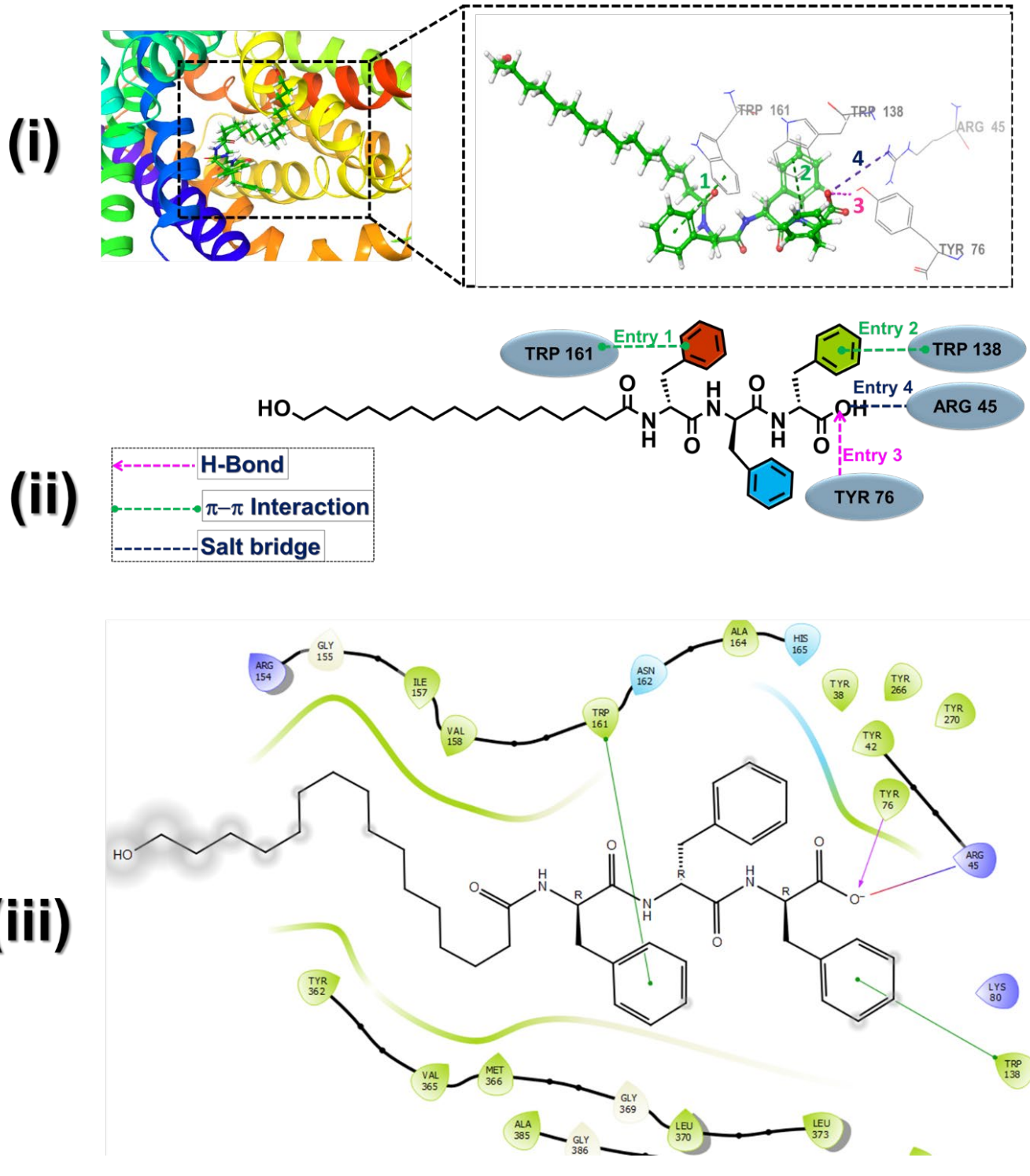

Figure S11:

i) 3D representation of the mode of interactions in Compound **I**
ii) Pictorial diagram of the mode of interactions in Compound **I**
iii) 2D representation of the mode of interactions in Compound **I**

C) 16-HPA-L-Phe-L-Phe-L-Phe-OH (compound-II)

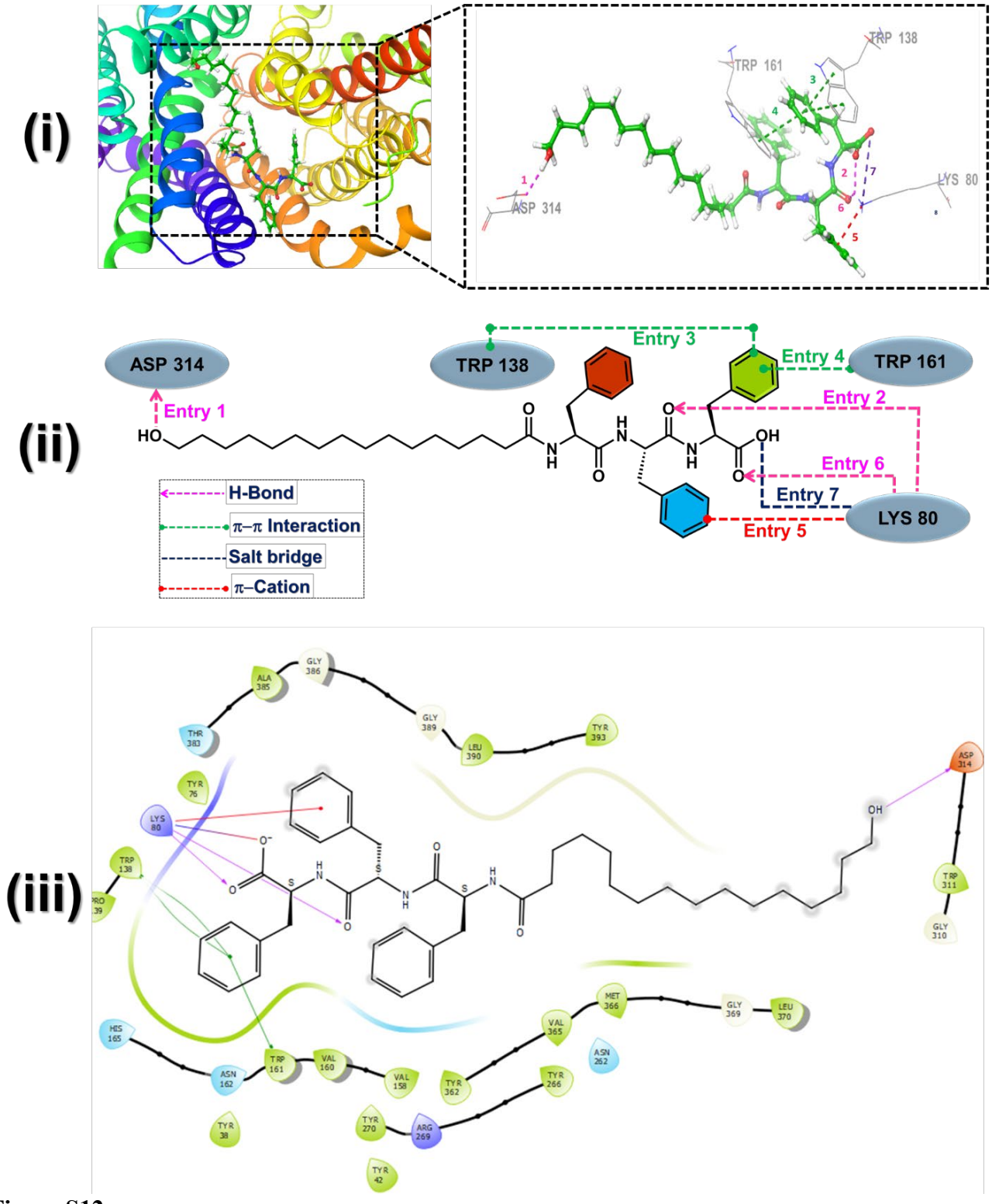

Figure S12:

i) 3D representation of the mode of interactions in Compound **II**
ii) Pictorial diagram of the mode of interactions in Compound **II**
iii) 2D representation of the mode of interactions in Compound **II**

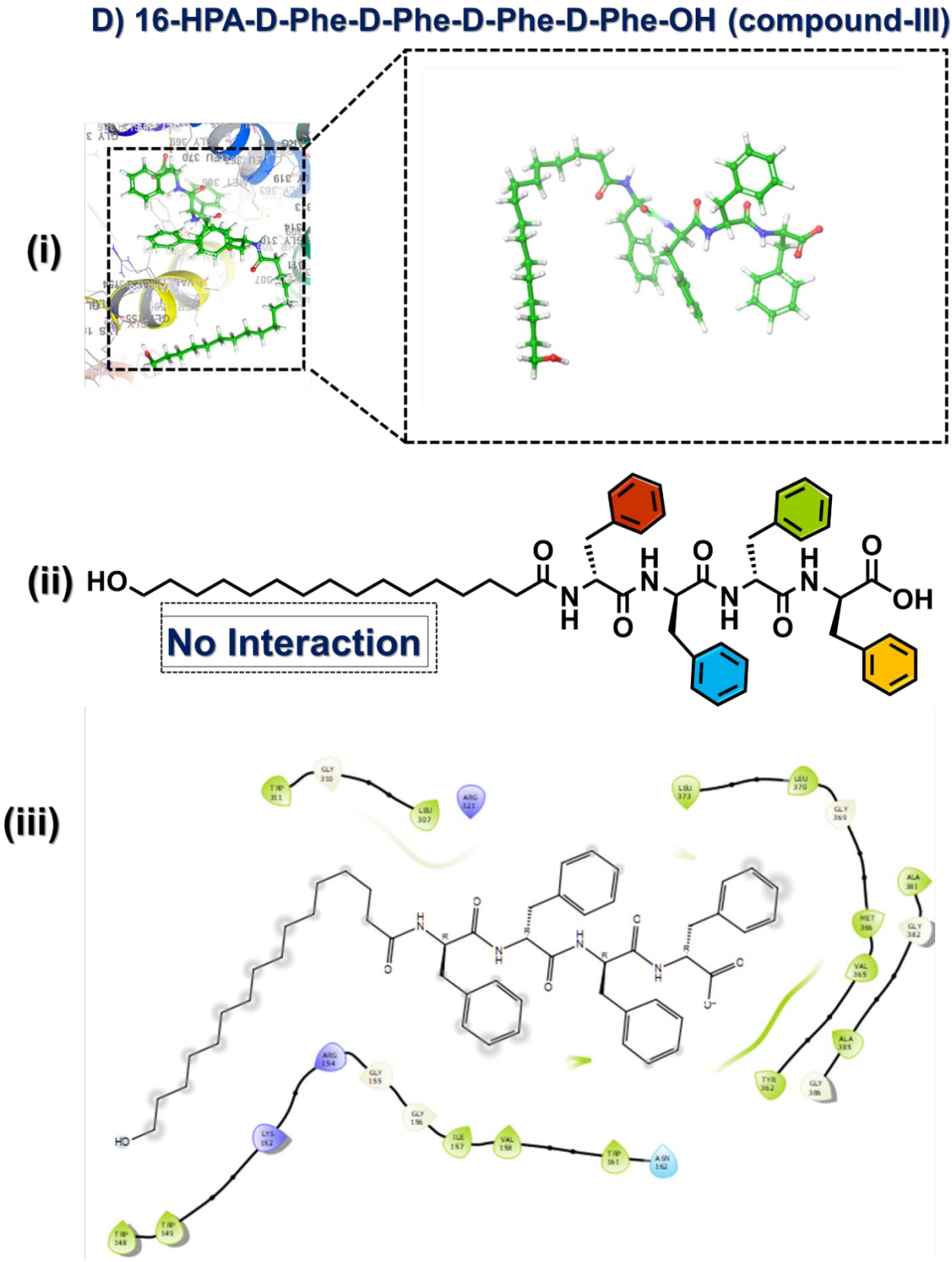

Figure S13:

i) 3D representation of the mode of interactions in Compound **III**
ii) Pictorial diagram of the mode of interactions in Compound **III**
iii) 2D representation of the mode of interactions in Compound **III**

E) 16-HPA-D-Phe-D-Phe-OH (compound-IV)

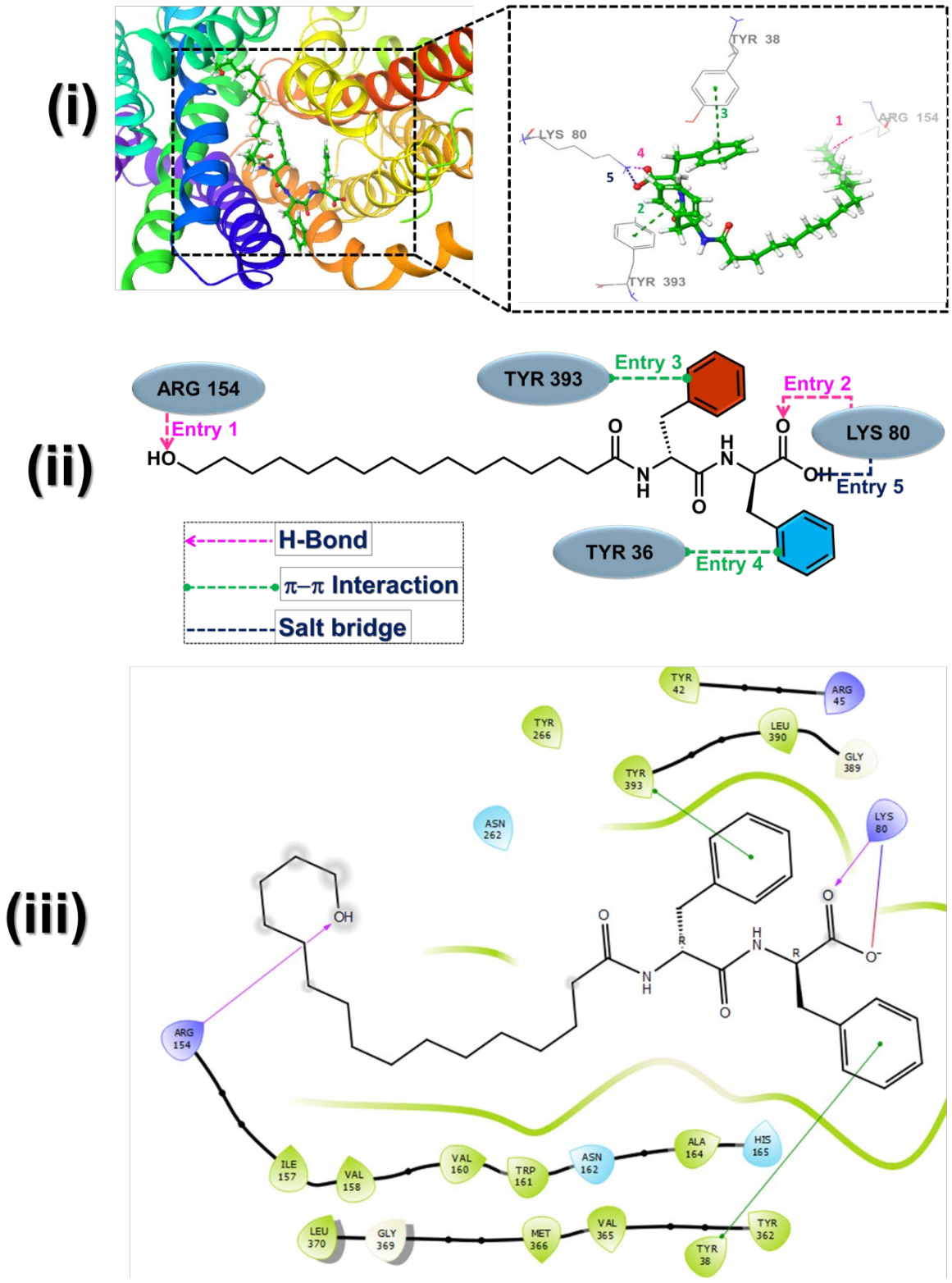

Figure S14:

i) 3D representation of the mode of interactions in Compound **IV**
ii) Pictorial diagram of the mode of interactions in Compound **IV**
iii) 2D representation of the mode of interactions in Compound **IV**

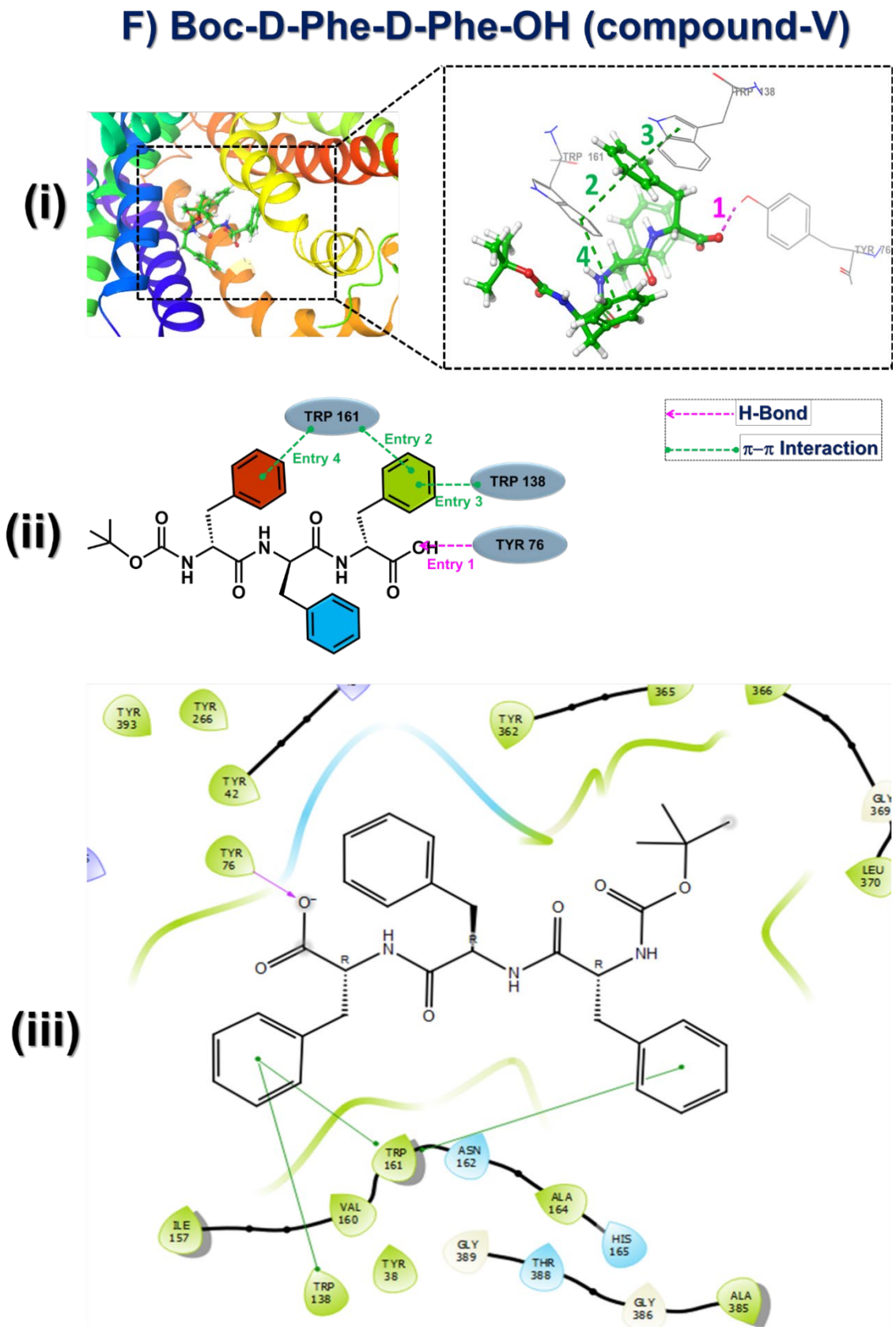

Figure S15:

i) 3D representation of the mode of interactions in Compound **V**
ii) Pictorial diagram of the mode of interactions in Compound **V**
iii) 2D representation of the mode of interactions in Compound **V**

TABLE S2: - Interactions of the Standard Drug Capecitabine and Compounds **I - V**

S. No.	Molecule Name	Nature of interactions	Interactions residues		Docking score	Binding energy Kcal/mol
			Donor	**Acceptor**		
1	**Capecitabine**	H-bond	TRP 161 NH	CO of Capecitabine	**-5.336**	**-50.17**
2		H-bond	ASN 162 NH	Aromatic ring CO		
3		H-bond	C_2 -OH of furan ring	ASN 162 CO		
			Donor	**Acceptor**		
1	**Compound I**	π–π	Phe(1)aromatic ring	TRP 161 aromatic ring	**-8.094**	**-55.29**
2		π–π	Phe(3)aromatic ring	TRP 138 aromatic ring		
3		H-bond	OH of TYR 76	Phe (3) O^- of COOH		
4		Salt bridge	NH of ARG 45	Phe(3) O^- of COOH		
			Donor	**Acceptor**		
1	**Compound II**	H-bond	16 HPA (OH)	CO of ASP 314	**-8.898**	**-47.84**
2		H-bond	LYS 80 Side chain of NH	Phe (2) CO		
3		π–π	Phe(3)aromatic ring	TRP 138 aromatic ring		
4		π–π	Phe(3)aromatic ring	TRP 161 aromatic ring		
5		π-cation	Phe(2)aromatic ring	LYS 80 Side chain of NH		
6		H-bond	LYS 80 Side chain of NH	Phe (3) CO		
7		Salt bridge	LYS 80 Side chain of NH	Phe(3) O^-		
			Donor	**Acceptor**		
1	**Compound III**	-	-	-	**-7.252**	**-63.16**
			Donor	**Acceptor**		
1	**Compound IV**	H-bond	ARG 154 aromatic ring of NH	16HPA (OH)	**-8.820**	**-65.28**
2		H-bond	LYS 80 Side chain of NH	Phe (1) CO		
3		π–π	Phe(1)aromatic ring	aromatic ring of TYR 393		
4		π–π	Phe(2)aromatic ring	aromatic ring of TYR 38		
5		Salt bridge	LYS 80 Side chain of NH	Phe(2) O^- of COOH		
			Donor	**Acceptor**		
1	**Compound V**	π–π	Phe(1)aromatic ring	Aromatic ring of TRP 161	**-8.721**	**-55.72**
2		π–π	Phe(3) aromatic ring	Aromatic ring of TRP 161		
3		π–π	Phe(3)aromatic ring	Aromatic ring of TRP 138		
4		H-bond	TYR 76	Phe(3) O^- of COOH		

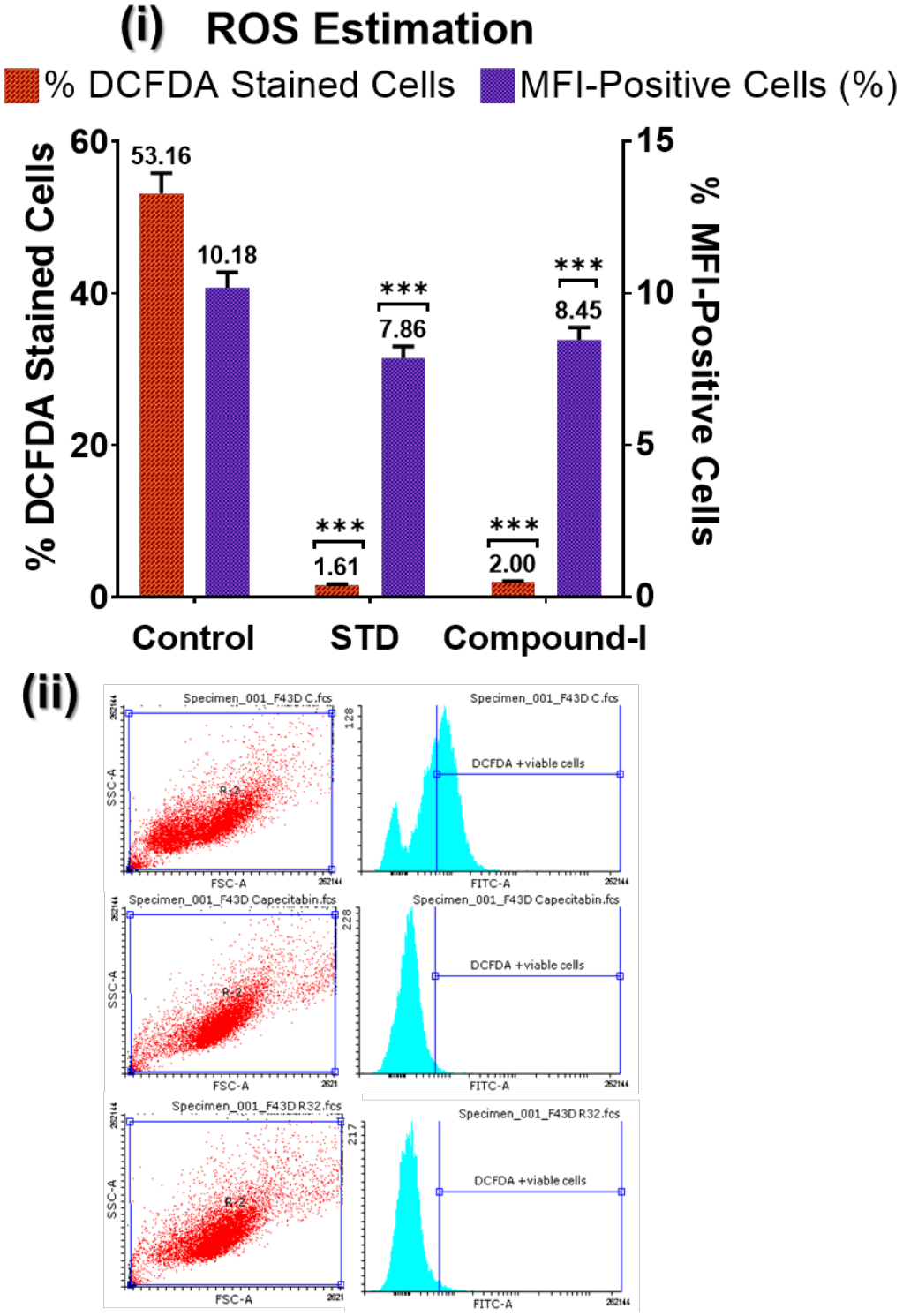

Figure S16 (i) Enlarged Graphical representation of Reactive Oxygen species of Control(untreated); Capecitabine (Standard); Compound **I** using DCFDA as the fluorescent probe and flow cytometric method (ii) Flow cytometric data of the above analysis estimation of % DCFDA Stained Cells w.r.t Control**.** Data was statistically analysed using a two-tailed paired Student's t test and presented as mean ± SD (N = 3). ***p<0.001, as compared to the control group

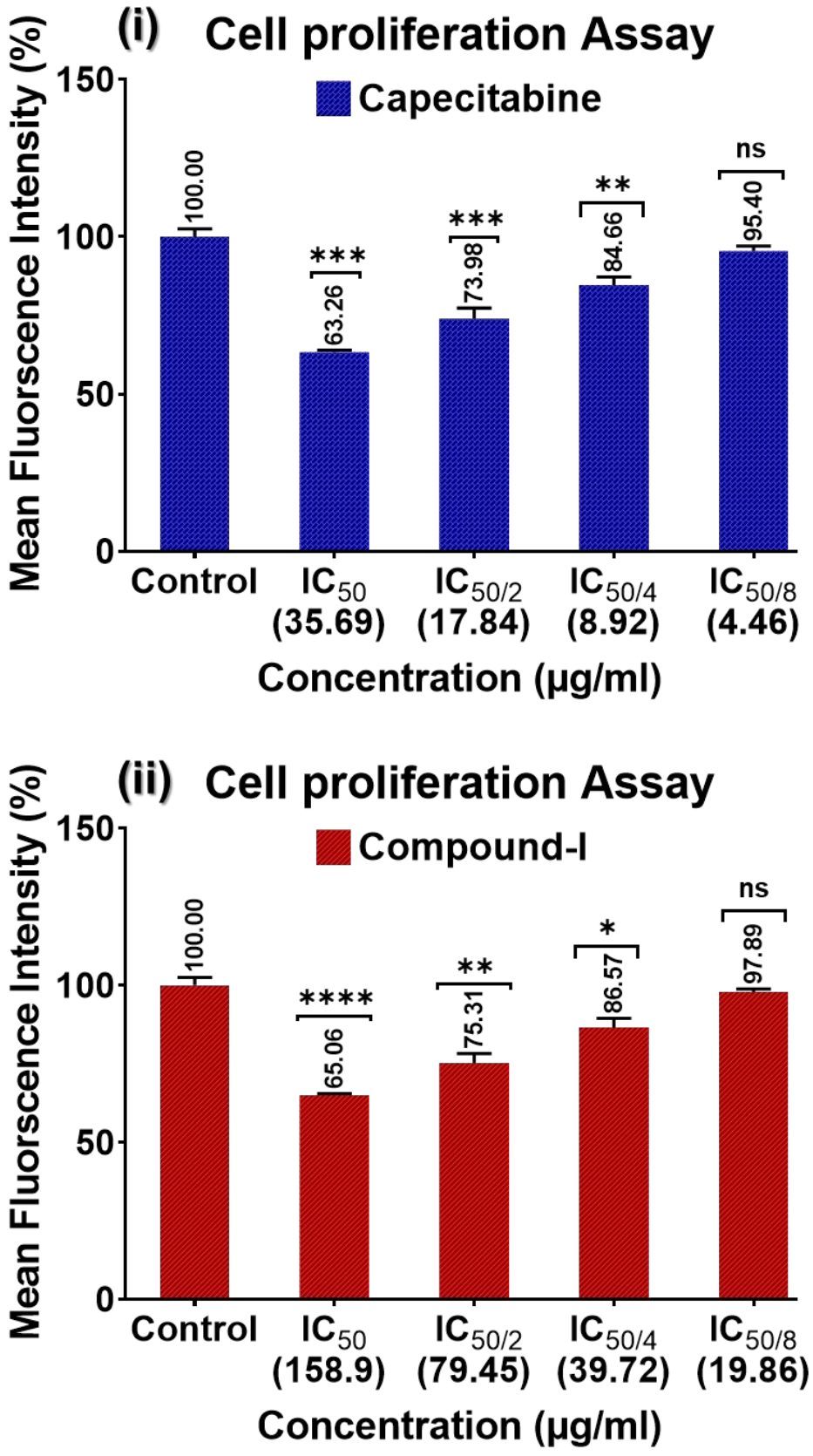

Figure S17: Cell Proliferation Assay of Compound **I** w.r.t Control group at different concentrations. Data was statistically analysed using a two-tailed paired Student's t test and presented as mean ± SD (N = 3). ns = not significant, *p<0.05, **p<0.01, ***p<0.001 and ****p < 0.0001, as compared to the negative control group

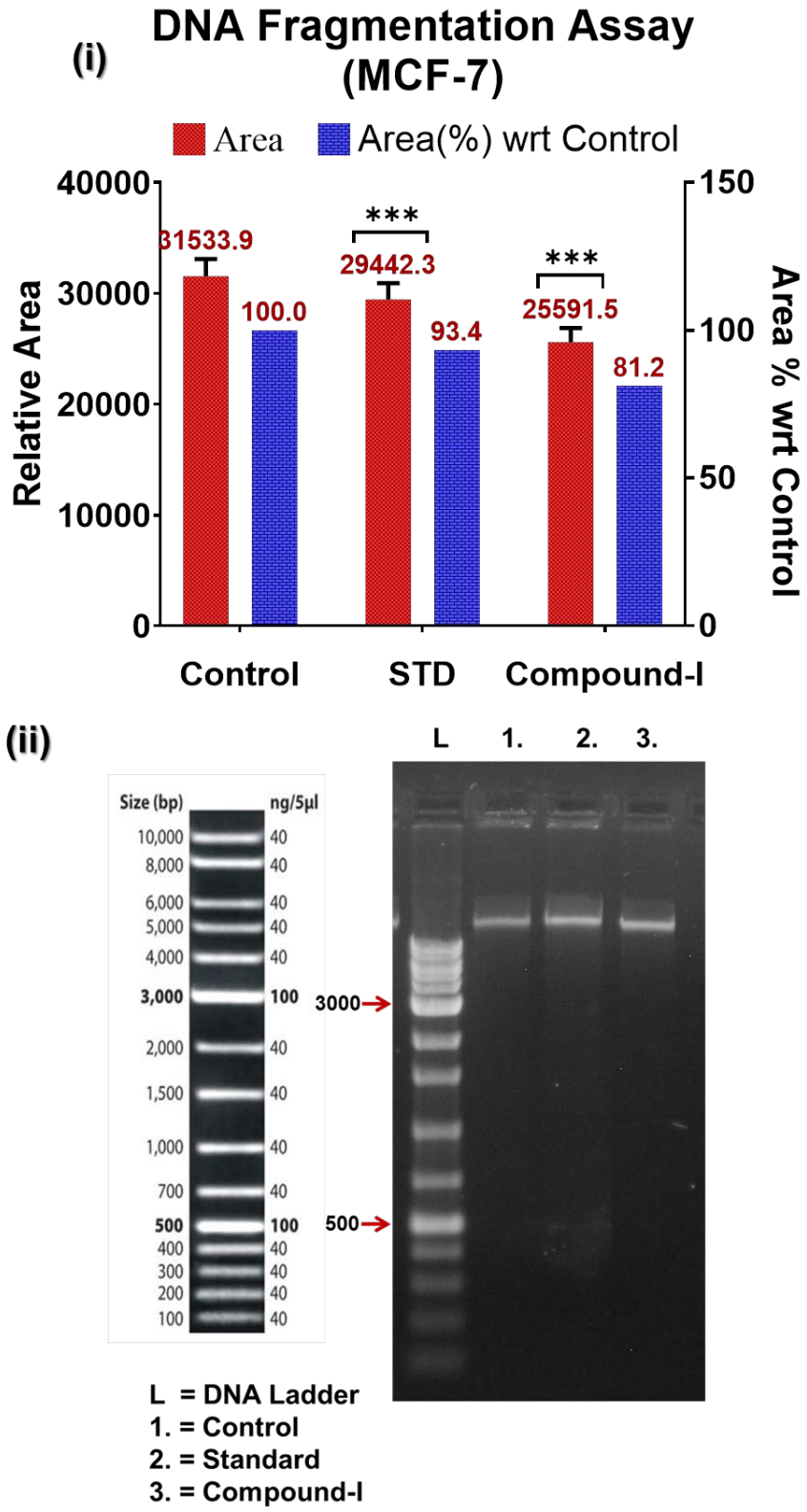

Figure S18 (i) Enlarged DNA Fragmentation assay of Compound **I** in MCF 7 Cell line; **(ii)** DNA ladder formation. From left Lane 1: Control, Lane 2 & 3 cells treated with standard drug Capecitabine and Compound **I**. Data was statistically analysed using a two-tailed paired Student's t test and presented as mean ± SD (N = 3), ***p<0.001, as compared to the control group.

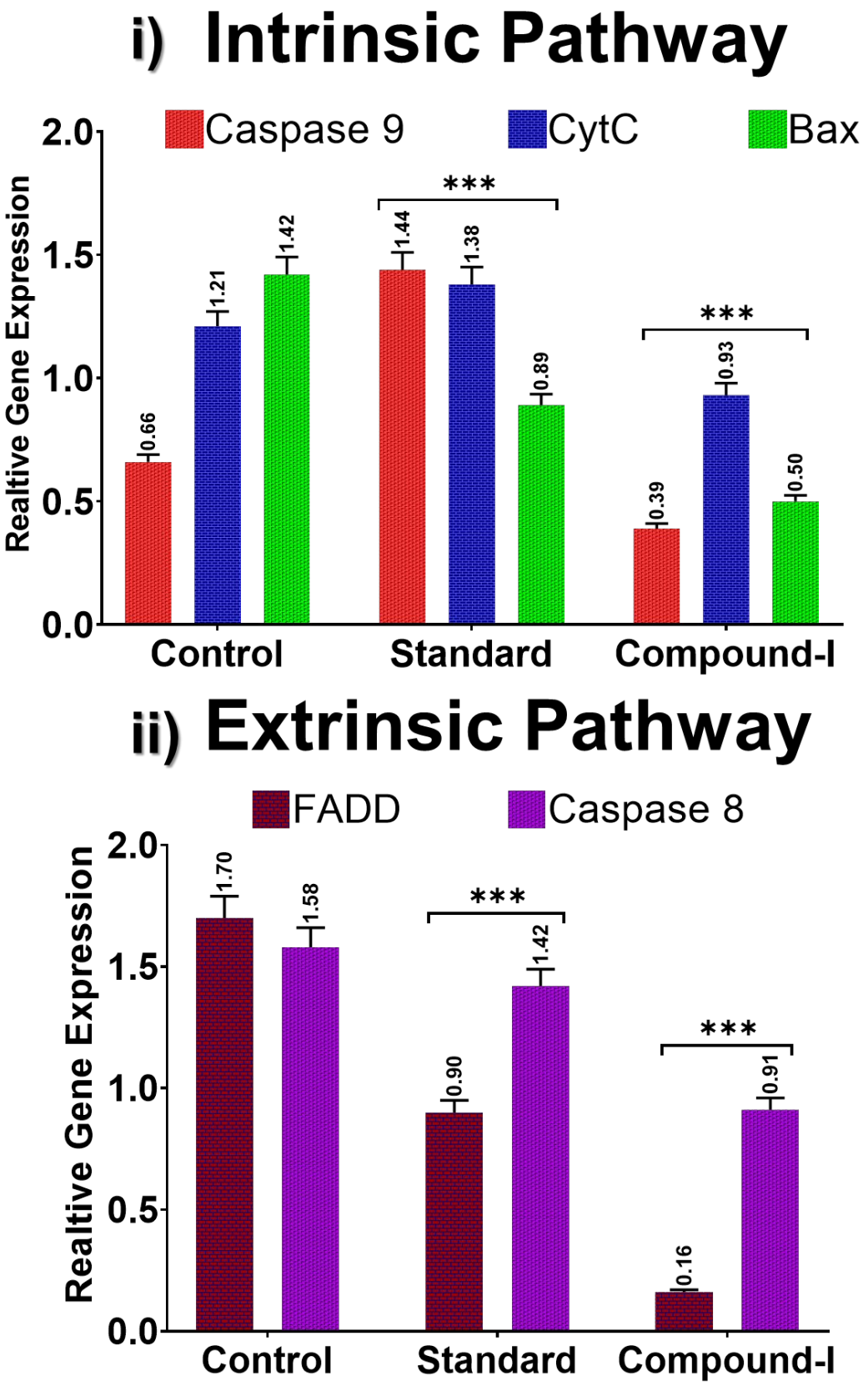

Figure S19 – (i-ii) Enlarged Relative gene expression data as measured by PCR to measure the effects of Compound **I** on apoptotic transcripts. Data was statistically analysed using a two-tailed paired Student's t test and presented as mean ± SD (N = 3), ***p<0.001 as compared to the control group

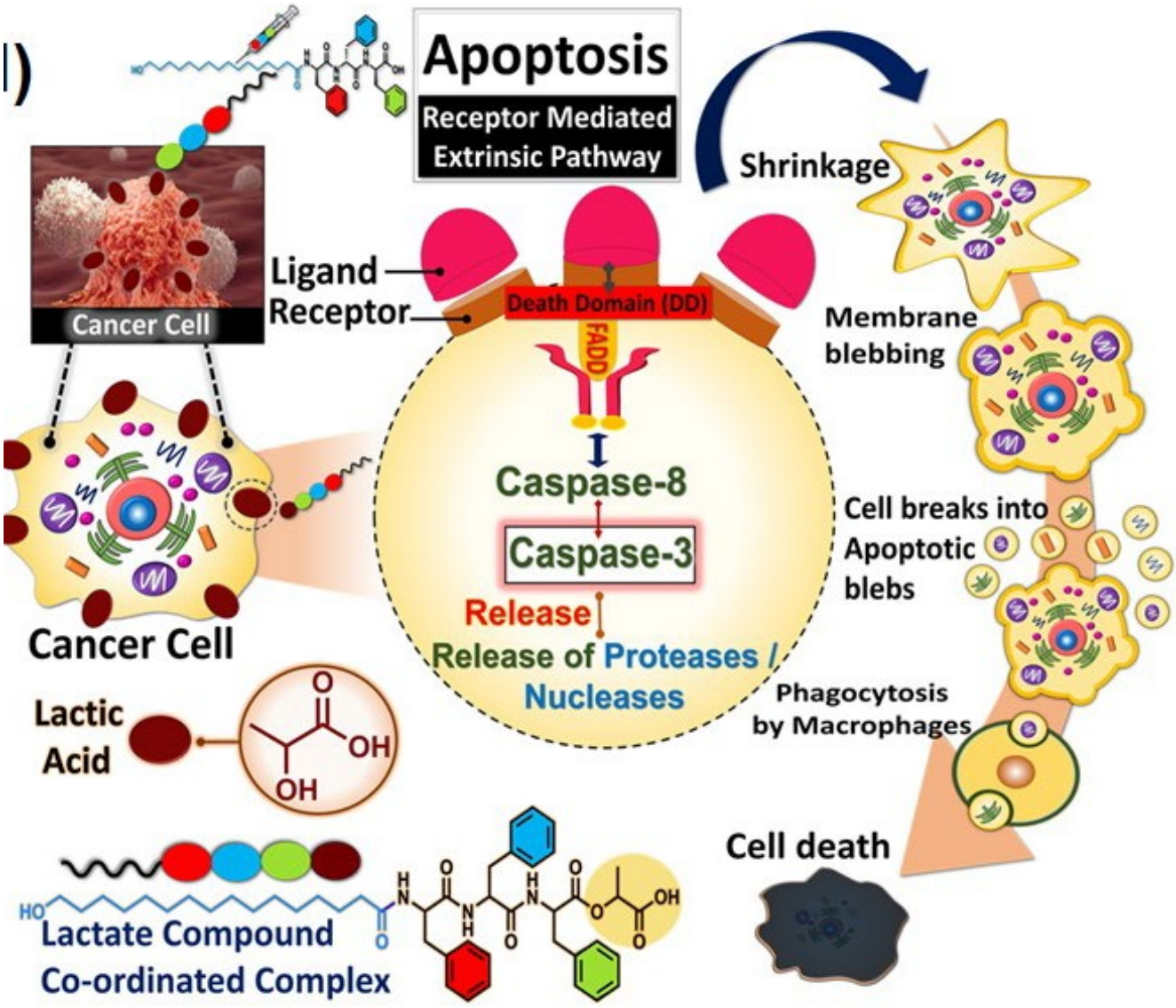

Figure S20: Enlarged apoptosis mechanism

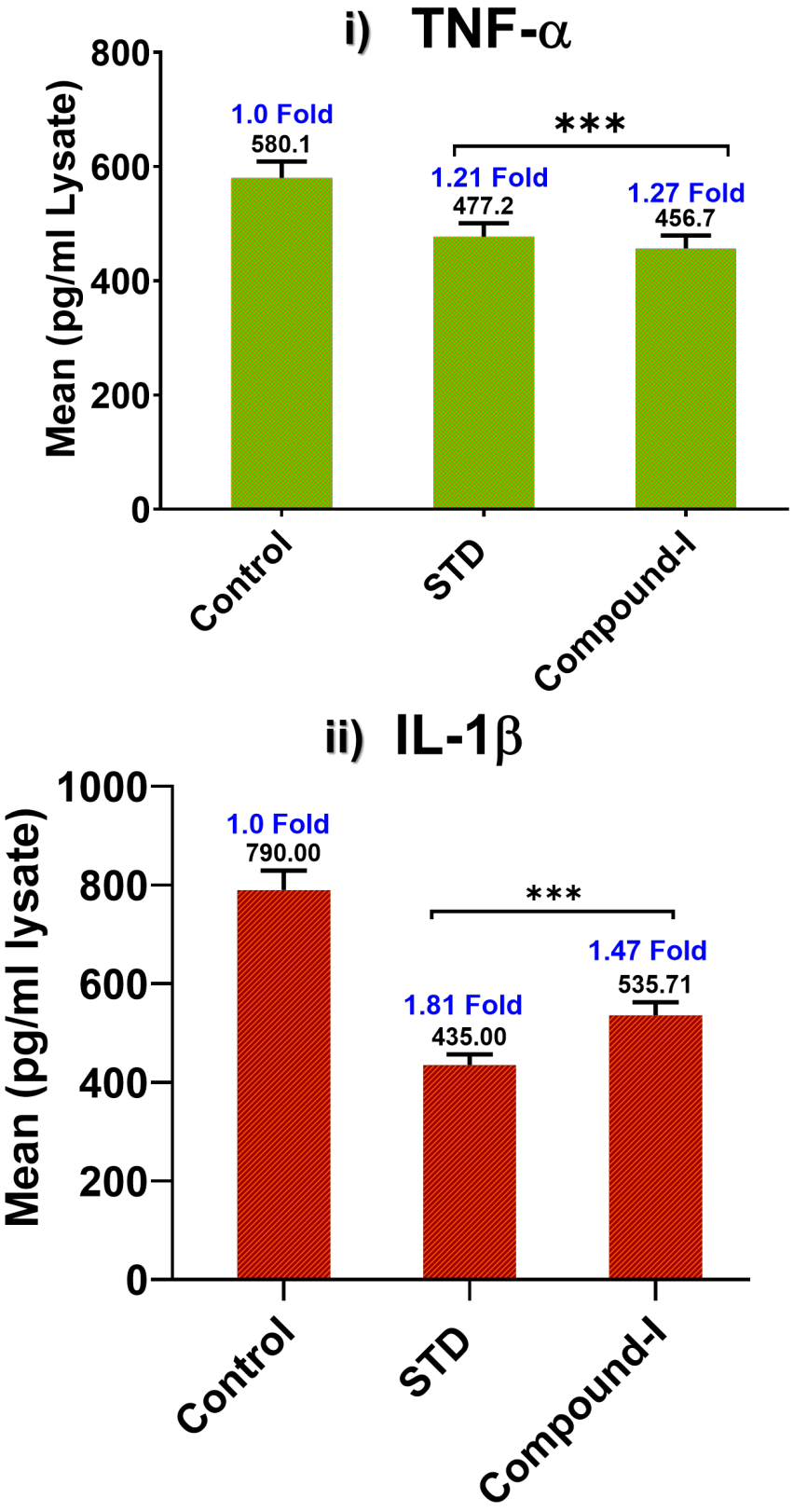

Figure S21– Enlarged Pro-inflammatory cytokines, **(i)** TNF-α, and **(ii)** IL-1β in LPS stimulated MCF-7 cells. Data was statistically analysed using a two-tailed paired Student's t test and presented as mean ± SD (N = 3). ***p<0.001 as compared to the control group.

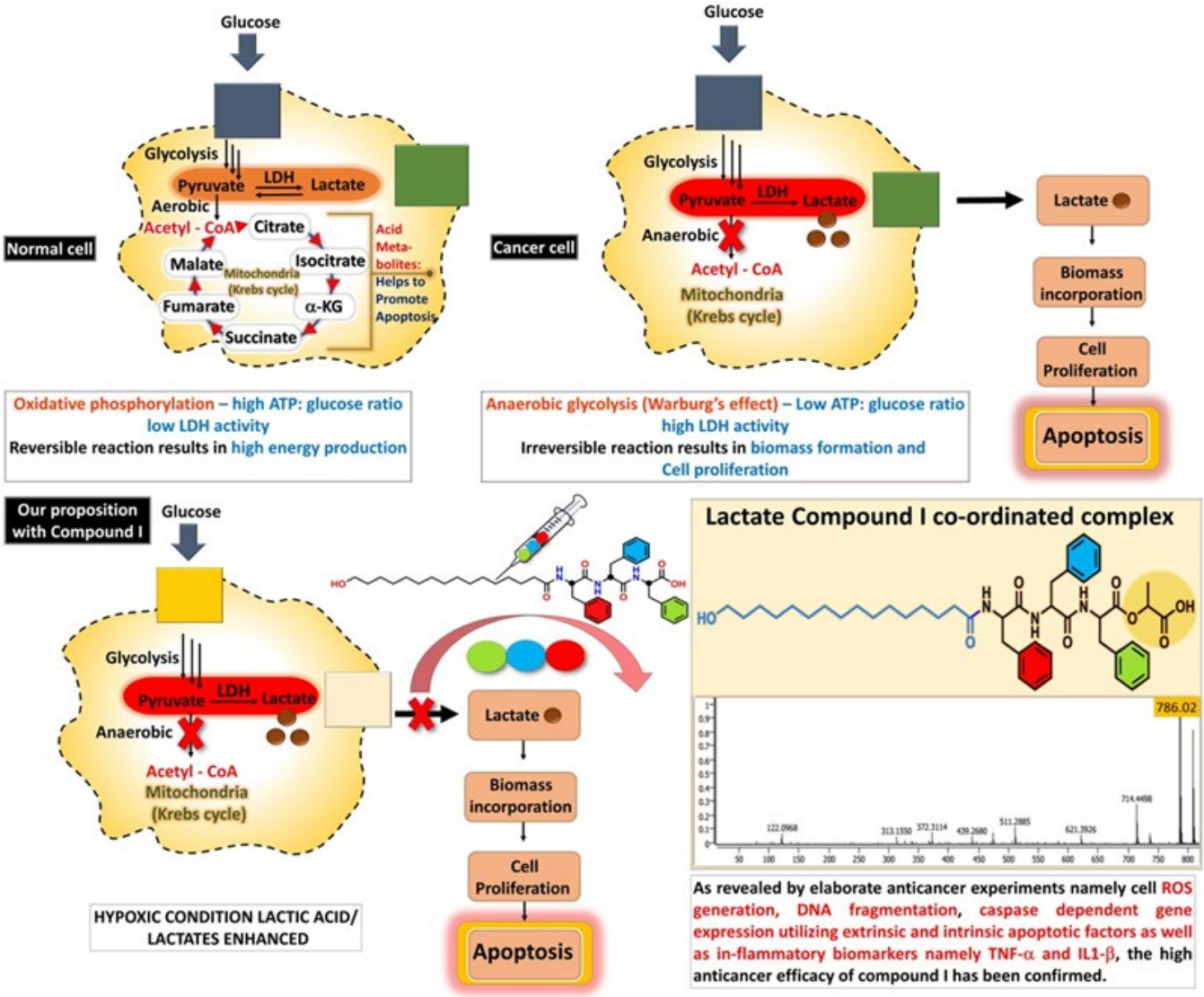

Figure S22: Probable Mechanism of our Proposed Solution given in the manuscript.

Anticancer Activity:

To explain the proposed mechanism of Anticancer Activity basic understanding of the working principle in a Normal Cell as well as in Cancerous Cell seems essential.

Primarily, interconversion of Glucose to Pyruvate, in our body, is a natural phenomenon due to glycolysis, which under aerobic conditions in Mitochondria forms Acetyl CoA, that initiates the Kreb's cycle and releases various metabolites such as citrates, isocitrates, α-keto glutarates, succinate, fumarates, malates and others that help the body's normal defense mechanism against various diseases (Figure S22, Normal Cell). [1] However a reversible mechanism operates where the pyruvate gets converted to Lactates/Lactic Acids , using the Lactate Dehydrogenase Enzyme (LDH), that gets tethered to the MCT Receptor, leading to normal cell metabolism (Figure S22, Normal Cell).

However, in cancerous cells under HYPOXIC conditions (anaerobic condition) the equilibrium of interconversion of pyruvate to lactate becomes unidirectional, leading to the accumulation of more amount of lactates/lactic acid. Thus mitocondria fails to function properly, leading to minimal interconversion of pyruvate to Acetyl CoA, eventually negligible initiation of Kreb's cycle. Henceforth the question of formation of the acid metabolites doesnot occur (Figure S22, Cancer Cell).[2]

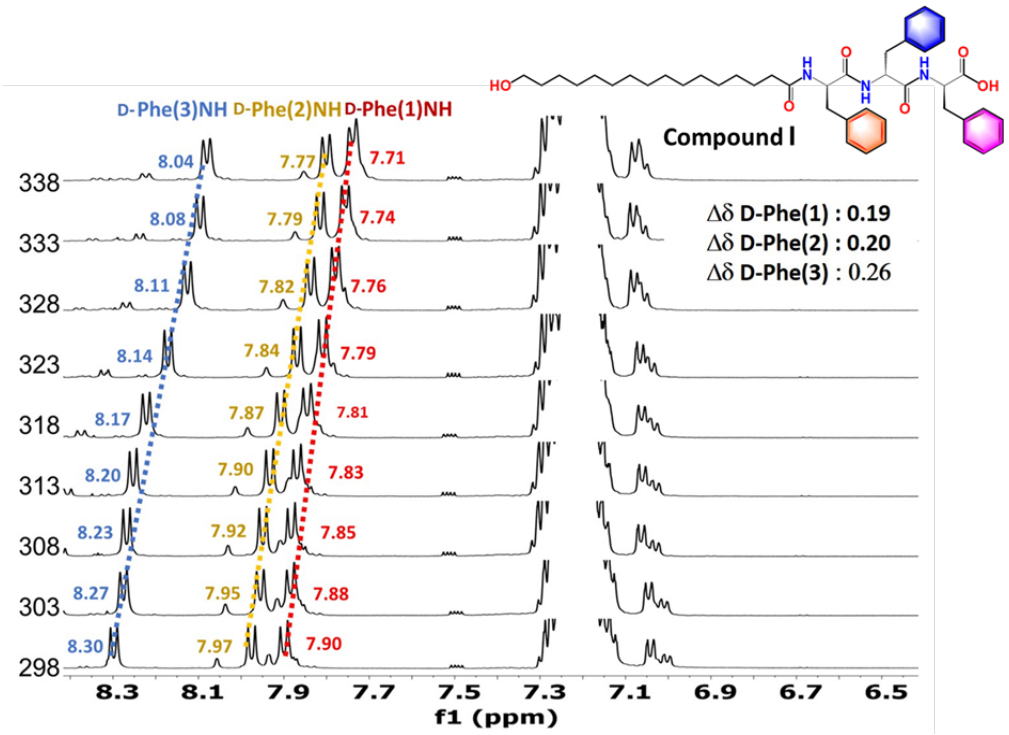

Figure S23 -Variable Temperature Dependent NMR study of Compound **I.** The change in chemical shifts Δδ oϕ Δ–Phe(1): 0.19; D-Phe(2):0.20 and D-Phe(3):0.26.

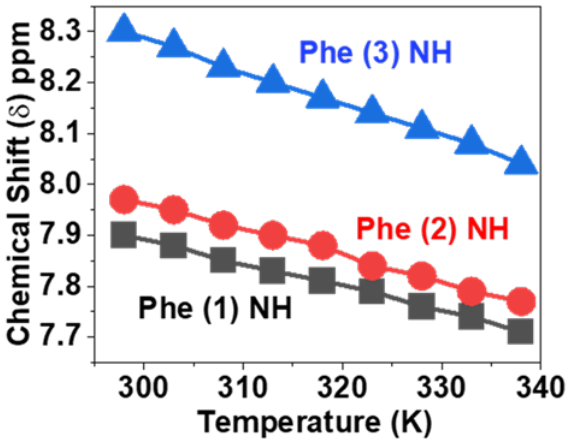

Figure S24– Plot of the NH chemical shifts of Variable Temperature dependent NMR of **Compound I**

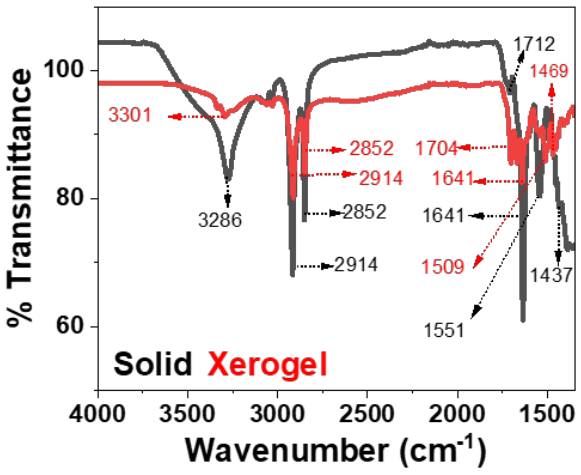

Figure S25 –FTIR Spectra of Compound **I: Solid & Xerogel**

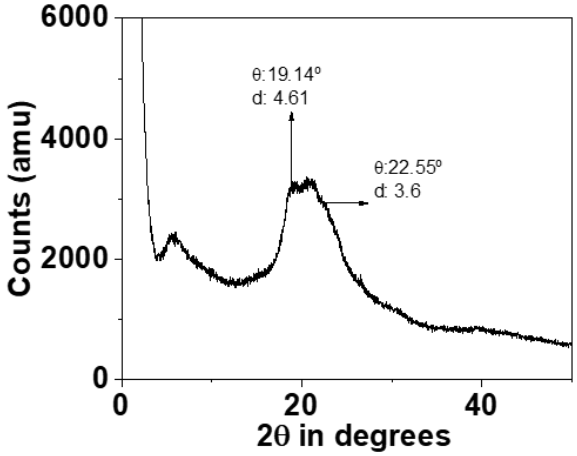

Figure S26 – Powdered X-Ray Diffraction spectra of the Compound **I**

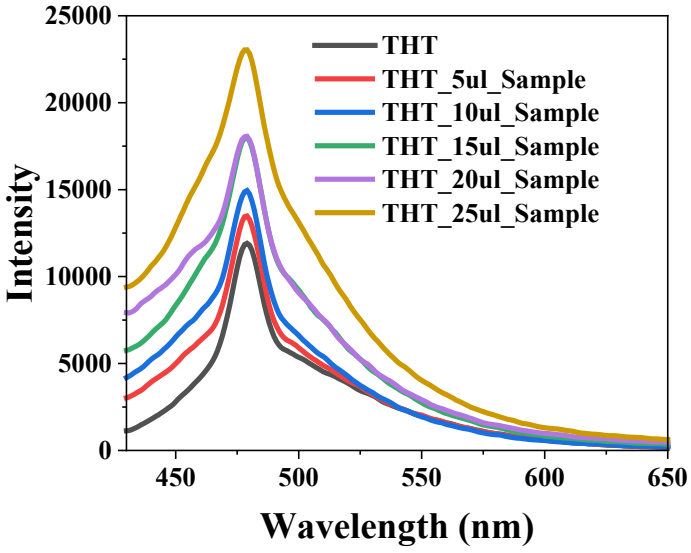

Figure S27: Thioflavin T assay, indicating enhancement of fluorescence signal on treatment with different concentration of compound **I** confirming amyloidogenic behaviour.

To test whether the self-assembled nanofibrillar structures of compound I, displayed amyloidogenic behaviour, we studied the Thioflavin T (ThT) binding assays. ThT is a dye which is believed to specifically interact with the cross β-sheet structure of amyloid fibrils, resulting in enhanced fluorescence emission at nearly 480 nm.[ref] As evident from **Figure S25**, the dye when treated with different concentration of the aged solution of compound **I**, indicated enhancement in fluorescence intensity in comparison to the drug alone, confirming amyloidogenic behaviour of compound **I**.

Actually, the inherent cytotoxic behavior of synthesized molecules are a function of its structure and physicochemical properties. However, the extent to which such structural aspects impact the mechanism of action of the molecule is the subject of our ongoing investigations and would be outside the scope of the present work. Although our *in vitro* studies do indicate the development of amyloidogenic behavior of compound I, the impact of such molecular self-assembly within a cellular environment would demand separate experimental strategies involving systematic investigations at the cellular levels. Hence at this point our focus states only to the inherent cytotoxic nature of the molecule with increase in concentration of the compound as reflected in the increase in cytotoxicity of MCF 7 and HEK293 cell lines in the MTT assay experiments.

Ref: S. Ray, A. K. Das, M. G. B. Drew and A. Banerjee *Chem. Commun*., **2006,** 4230–4232**.**

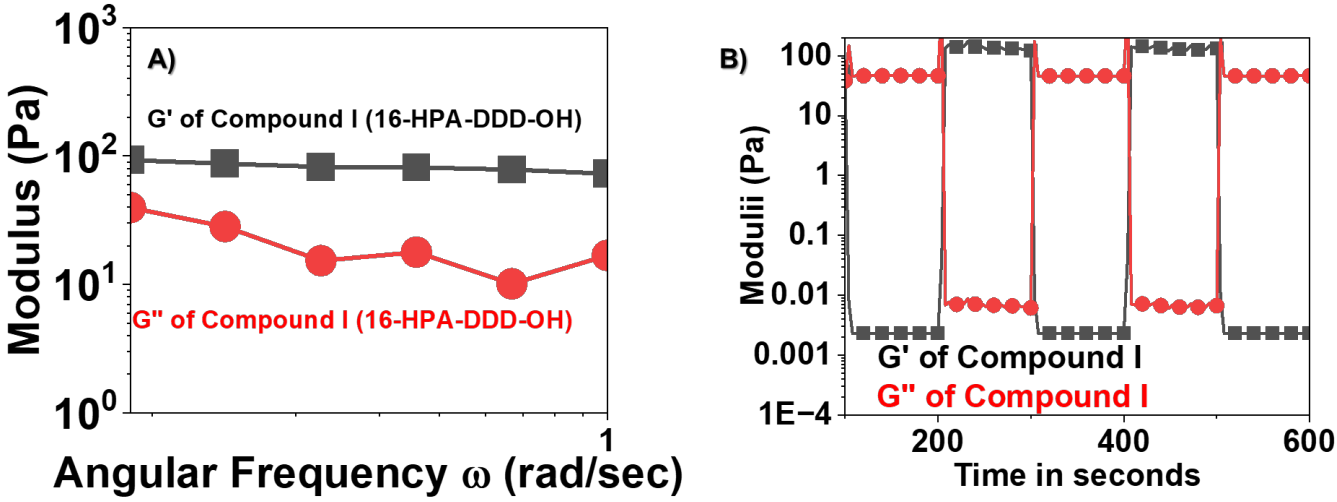

Figure S28. A) The Angular Frequency Curve of Compound **I**, showing the storage modulus to be higher than that of loss modulus; confirming hydrogel formation. B) Step-Strain experiments affirming the injectable property of Compound **I**.

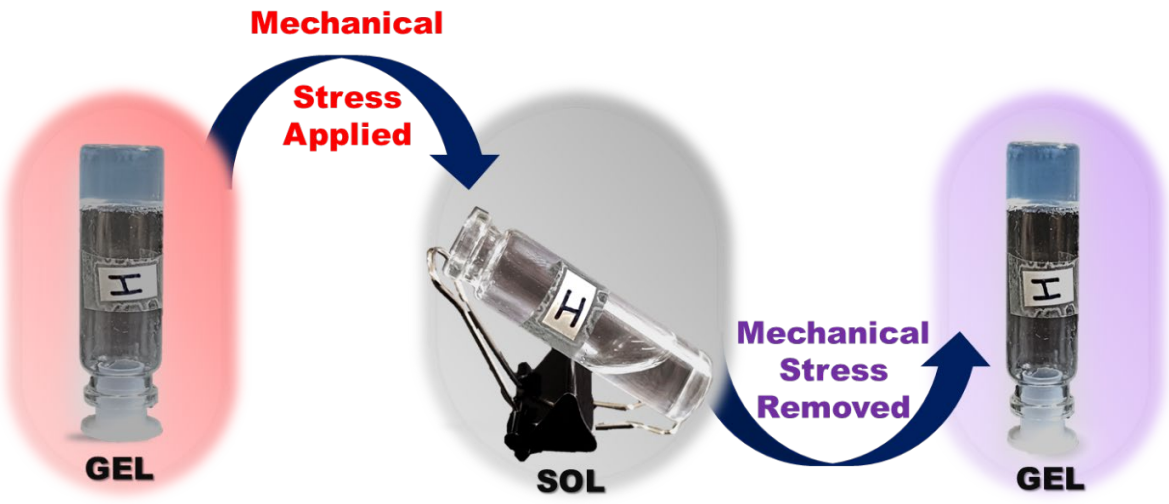

Figure S29– Photographic Images of Gel to Sol Transition and vice versa for Compound **I**

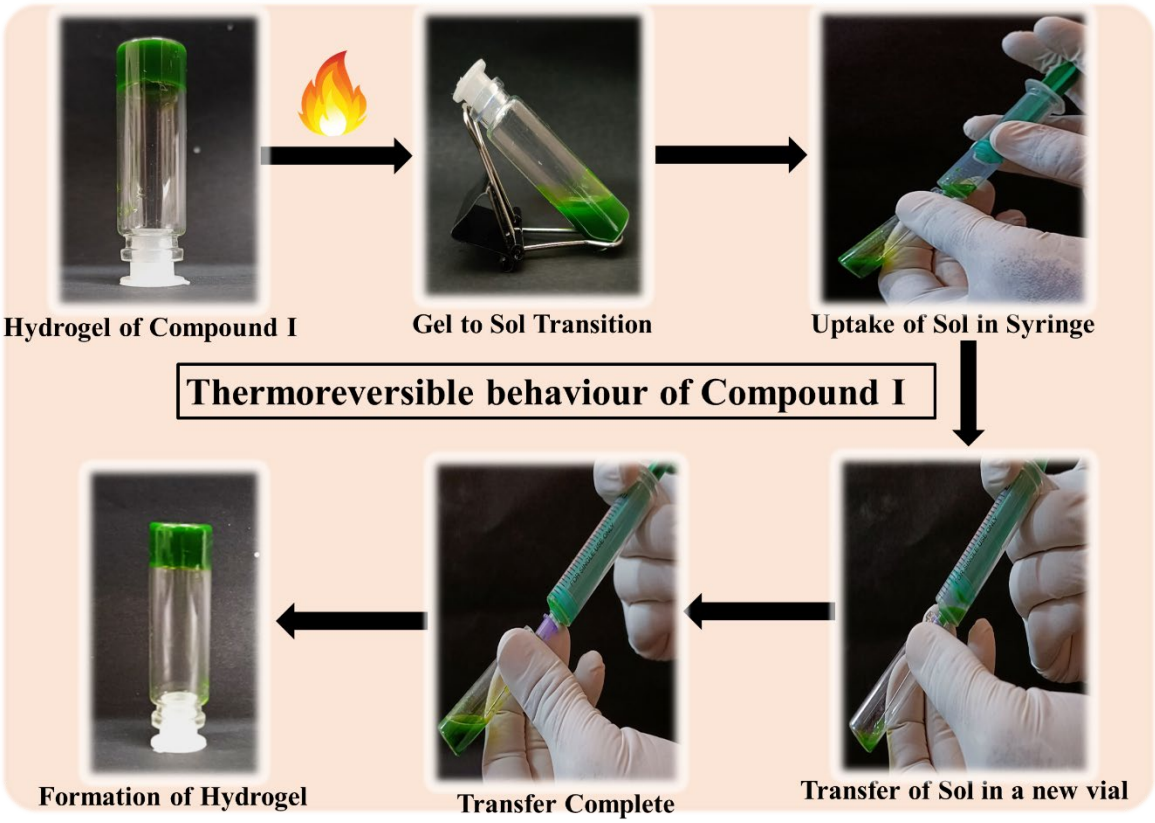

Figure S30- Phenomenon of Thermoreversibility in Compound **I**

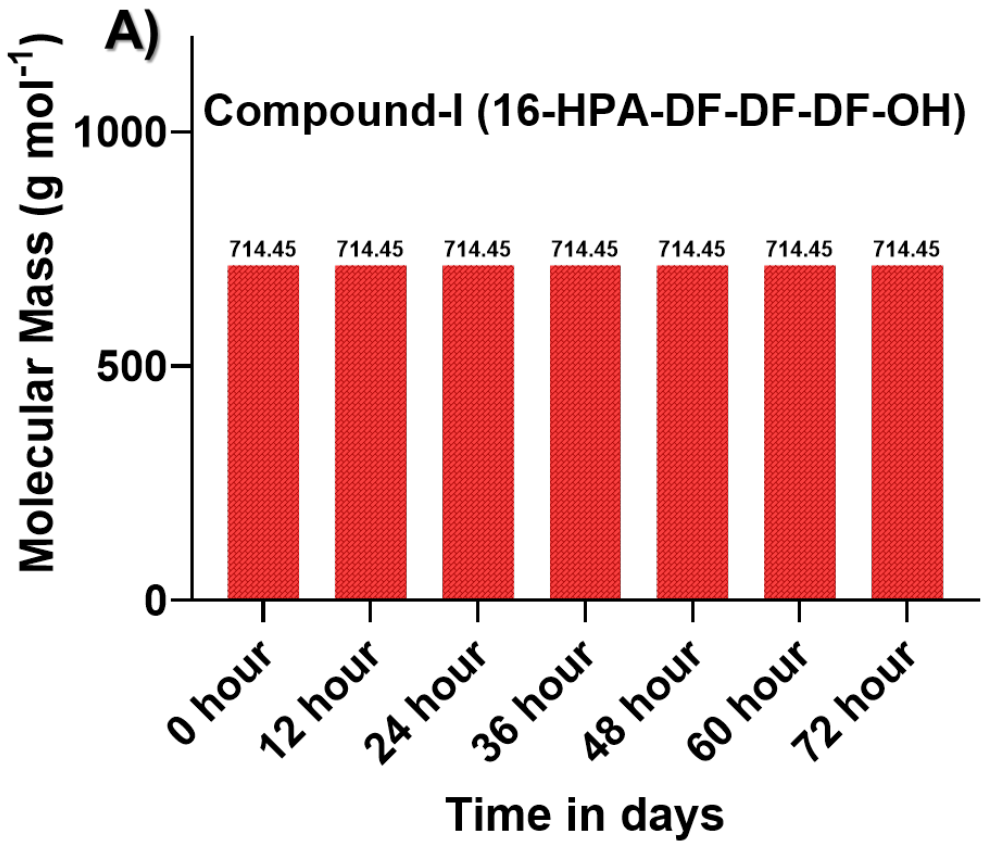

Figure S31: Enlarged Proteolytic degradation studies of Compound **I**, obtained after treatment of the compound with the proteolytic enzyme proteinase K for 72 hrs and recording its mass degradation.

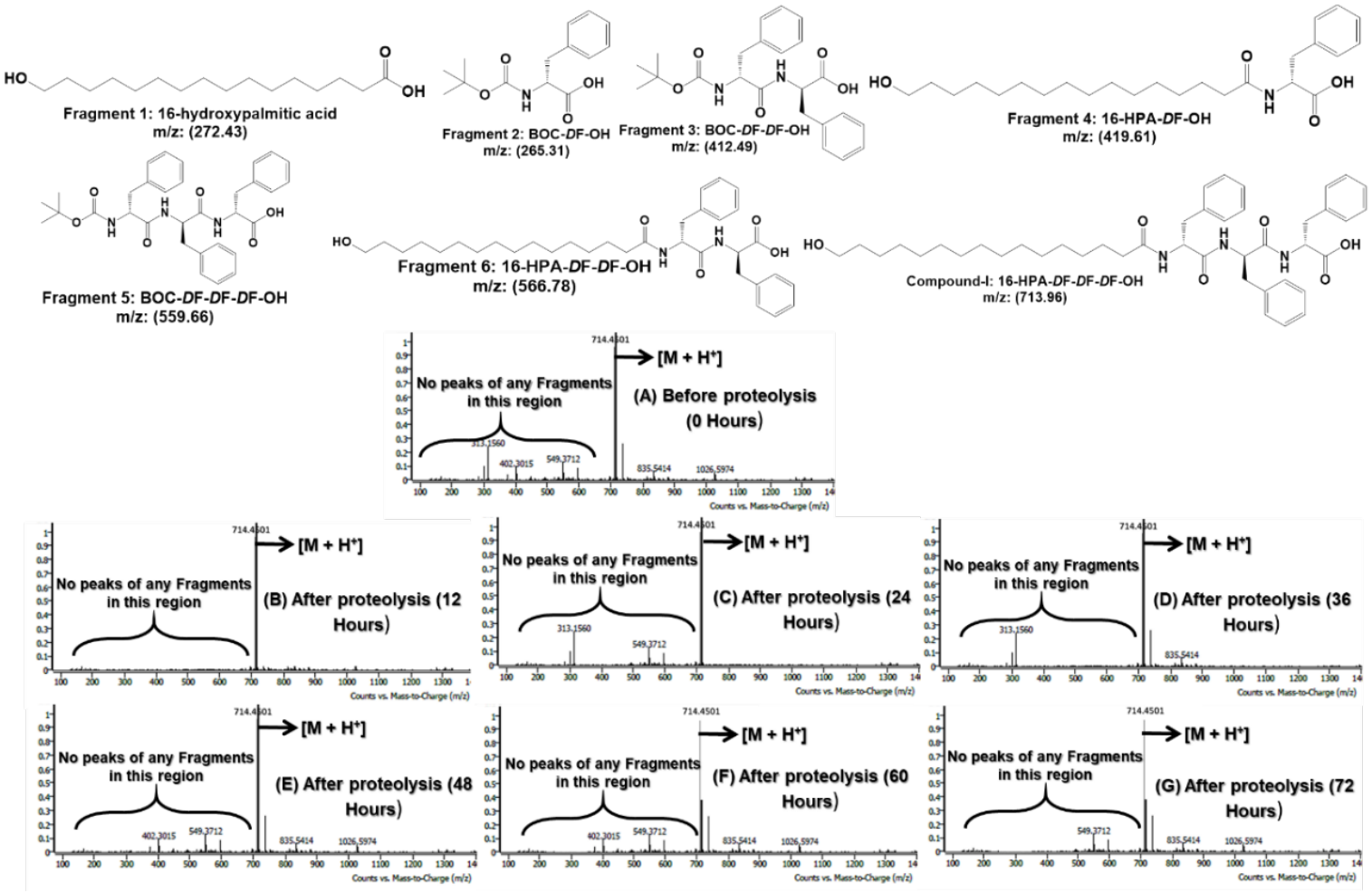

Figure S32: Structures of the possible fragments that could be obtained during the proteolytic experiments (top). Mass Spectra of Compound **I**, recorded at different time intervals of the Experiment **(A-G).**

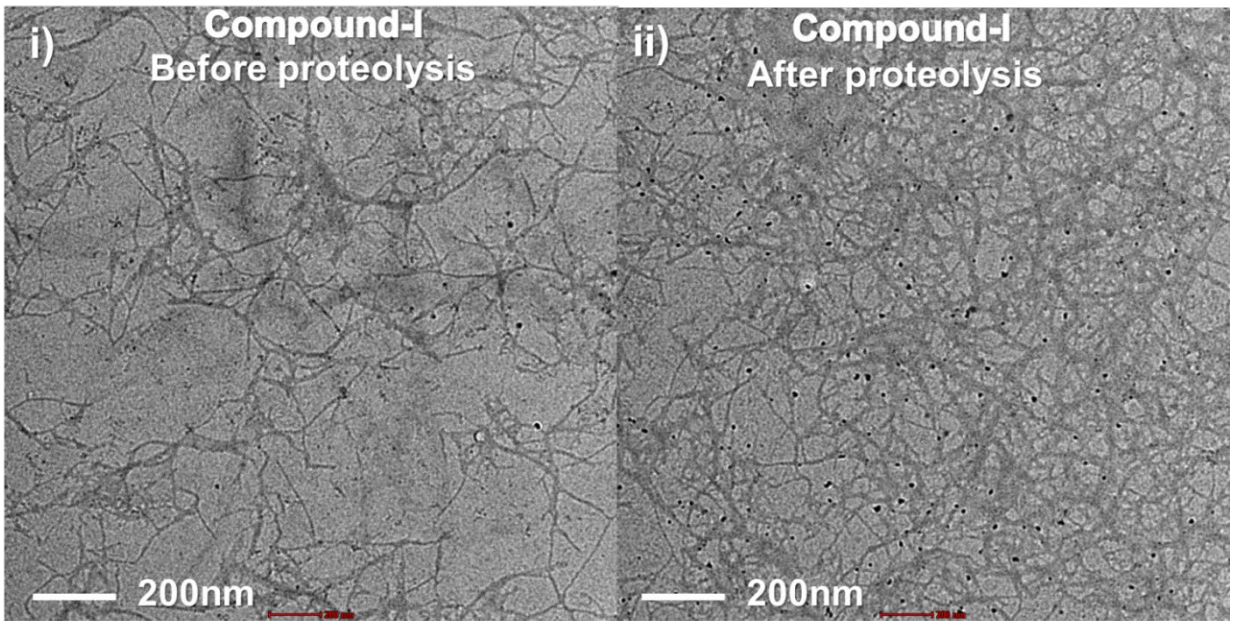

Figure S33 – TEM images of the compound showing the filamentous fibrillar network obtained before and after proteolysis of Compound **I**

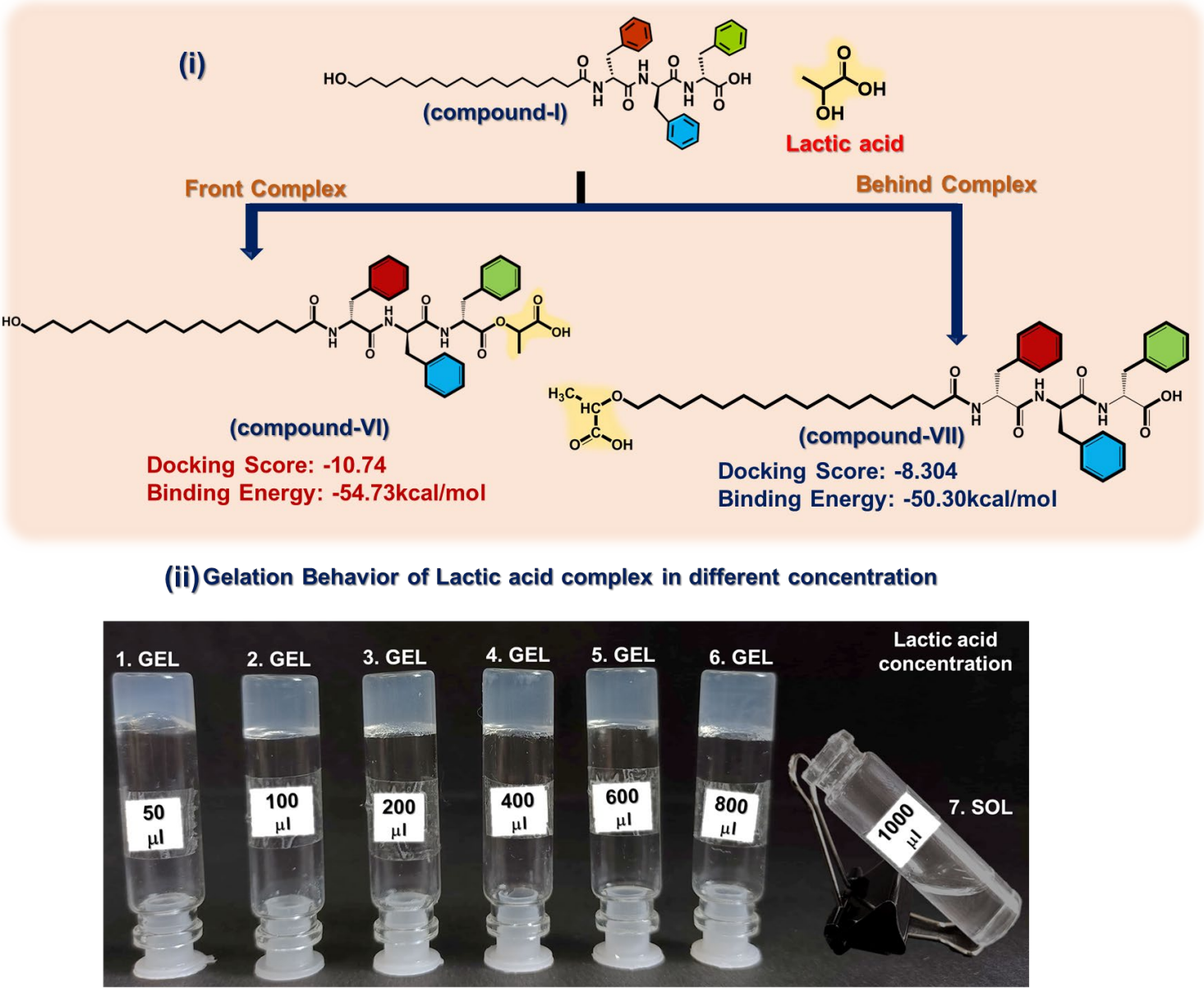

Figure S34: (i) Compound **I** form complex with Lactic acid from both side of its terminal either from Compound **VII** (Behind complex) or Compound **VI** (Front complex) showing different docking scores and binding energies; (ii) Gelation properties of Lactic acid complex molecules with different concentration

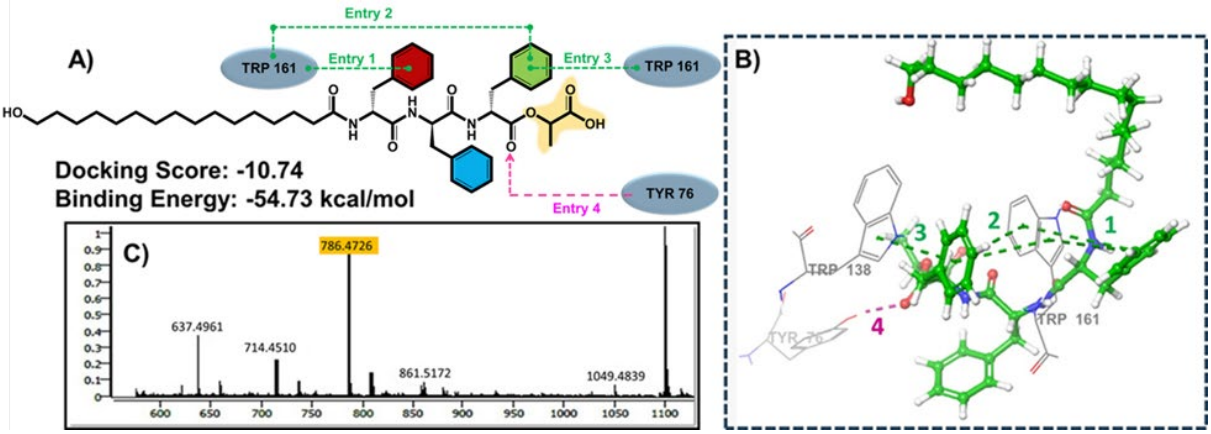

Figure S35– Docking studies of lactate Compound **I** co-ordinated complex with receptor MCT1 with Mass Spectra

i) 3D representation of the mode of interactions in Compound **VI**
ii) 2D representation of the mode of interactions in Compound **VI**
iii) Pictorial diagram of the mode of interactions in Compound **VI**
iv) Confirmation with Mass Spectrometry

Figure S36: Exploration of the Gelation properties of compound I with varied concentration (200µl, 400 µl and 600 µl) of a) citric acid and b) malic acid, indicating no gel formation, unlike lactic acid.

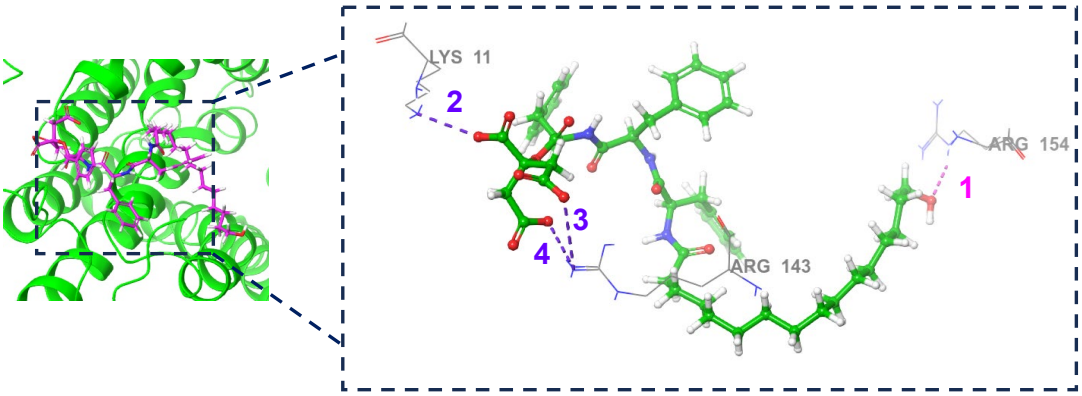

Figure S37– 3D representation of the mode of interactions of citrate co-ordinated Compound **I** complex with receptor MCT1

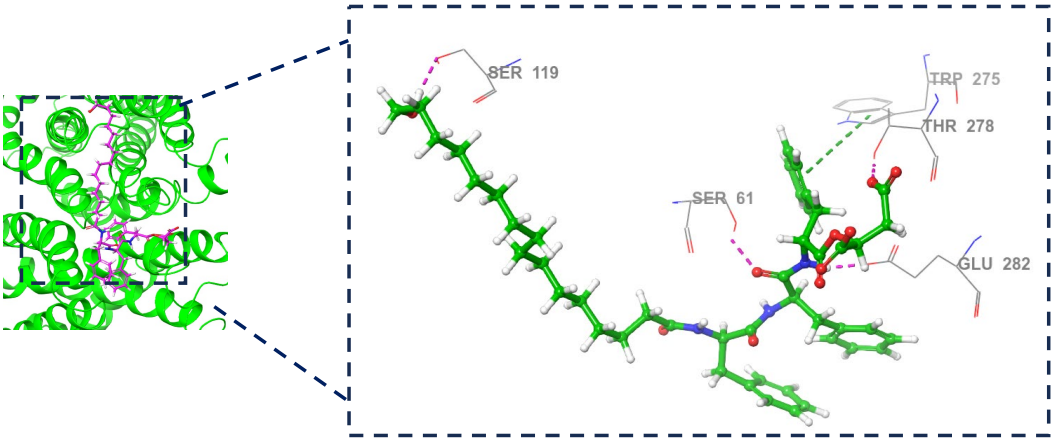

Figure S38-3D representation of the mode of interactions of malate co-ordinated Compound **I** complex with receptor MCT1 .

We still tried to check the gelation propensity, with the two metabolites namely a) citric acid and b) malic acid. Surprisingly, no gelation occurred in both the cases. (Figure S36-S38).To reaffirm our observation, we sought the help of docking studies and docked the citrate and malate derivatives of compound **I** in the receptor 1PW4, using the same constraints of compound **VI**. The docking score(DS) and binding energies (BE) are as follows: a) citrate : -5.30(DS); -18.86 Kcal/mol(BE); b) malate: -1.69(DS); -11.14 Kcal/mol(BE); [For comparison purpose the parameters of Compound VI (lactate complex): have also been given : -8.30(DS); -50.30 Kcal/mol(BE); Compound I(no complex formation) : -8.09(DS); -55.29 Kcal/mol(BE); Thus it is clearly evident that the DS and BE for lactate complex is much higher than citrate and malates, which could be the probable reason for no gel formation of these metabolites. **(Figure S36-S38)**

Ref 1: Arnold , Paige K ., Finley, Lydia W S. ***J Biol Chem*** **. 2023, 299,102838.**

Ref 2: MacLean, A., Legendre, F., & Appanna, V. D. (2023). ***Critical Reviews in Biochemistry and Molecular Biology*****,** ***58*****(1), 81–97.**